

Asymmetry assessment using cone-beam CT: a class I and class II patient comparison

A THESIS
SUBMITTED TO THE FACULTY OF THE GRADUATE SCHOOL
OF THE UNIVERSITY OF MINNESOTA
BY

Matthew Michael Sievers

IN PARTIAL FULFILLMENT OF THE REQUIREMENTS
FOR THE DEGREE OF
MASTER OF SCIENCE

Dr. Brent Larson

June 2010

© Matt Sievers DDS 2010

Acknowledgements

I would like to thank the people who have made this research project possible, including:

Dr. Brent Larson who provided invaluable guidance and wisdom, without which this thesis would not have been completed. Thank you for the time you spent meeting with me to discuss the details of this project and the time put into reading the manuscript and offering suggestions for improvement.

Dr. John Beyer who reviewed the manuscript and provided thoughtful feedback to improve its content.

Dr. Mansur Ahmad who reviewed the manuscript and provided thoughtful feedback to improve its content.

Andrew Wey and Philippe Gaillard, for their help in analyzing the data produced in this study as well as taking the time to meet with me to discuss the meaning of the statistical results.

Dedication

This thesis is dedicated to my parents, Ken and Sharon Sievers, who have always been tireless supporters as I worked towards my goals. I could not have been blessed with more loving parents.

To my wife Ashley, for her willingness to live apart while I completed this residency program and for her continuous love and support.

Abstract

Introduction: Asymmetry assessment is an important component of orthodontic diagnosis and treatment planning. Before the advent of three-dimensional imaging, orthodontists relied on two-dimensional headfilms to diagnose asymmetry. Cone beam computed tomography (CBCT) allows for assessment of asymmetry on a dimensionally accurate volumetric image. This study aims to determine if there is a difference in skeletal asymmetry between patients with a skeletal class I ANB angle compared to patients who have a skeletal class II using CBCT images. **Methods:** CBCT images were examined from 70 consecutive patients who presented for routine orthodontic care and fit inclusion criteria. Asymmetry was analyzed using an asymmetry index developed by Katsumata et al.¹⁸ Anatomic landmarks were defined and reference planes were established to determine the variance of the landmarks using a coordinate plane system. 30 randomly selected patients were reanalyzed to assess reliability of the method. **Results:** Statistical analysis demonstrated no significant relationship between asymmetry and ANB angle for any of the landmarks. Asymmetry index scores were reproducible within a certain range of agreement for each landmark. **Conclusions:** Based on this study, the differential in jaw proportion common for class II skeletal patterns results in no more skeletal asymmetry than class I skeletal patterns. Altman-Bland agreement plots suggest that some modification may be indicated to the system proposed by Katsumata et al¹⁸ to improve asymmetry diagnosis.

Table of Contents

	Page
Acknowledgements	i
Dedication	ii
Abstract	iii
Table of Contents	iv
List of Tables	v
List of Figures	vi
Introduction	1
• Etiology, Classification, and Treatment of Craniofacial Asymmetry	2
• Skeletal Asymmetry Relationship to Malocclusion	3
• Radiographic Asymmetry Assessment	4
• Previous Three-Dimensional Skeletal Asymmetry Analyses	6
• Landmark Identification with CBCT	8
• Linear Measurement Accuracy with CBCT	10
Aims, Objectives, Null Hypotheses	13
Materials and Methods	14
Statistical Analysis	34
Results	34
Discussion	44
• Possible Sources of Error	50
Conclusions	53
References	54

List of Tables

	Page
Table 1. Landmark definitions for asymmetry assessment	18
Table 2. Pearson Correlation Coefficients of ANB and landmarks across all patients	36
Table 3. ANOVA F and P values comparing mean asymmetry index score for each group at each landmark	39
Table 4. Comparing mean asymmetry index scores from the present study and previous study by Katsumata et al ¹⁸	39
Table 5. Pearson correlation coefficients comparing mean asymmetry index scores of original and repeat measures	40
Table 6. Altman-Bland summary data analyzing agreement between initial and repeat measures of asymmetry index.	40
Table 7. Boundaries for asymmetry and marked asymmetry diagnosis by landmark according to system used by Katsumata et al ¹⁸	48

List of Figures

	Page
Figures 1-14. Landmark Identification on various CBCT views	19-32
Figure 15. CBCT views of reference planes used in this study	33
Figure 16. Scatter plots of asymmetry index scores by ANB angle and landmark	36-38
Figure 17. Altman-Bland plots of agreement of asymmetry index scoring between the original data and the 30 patients who were re-assessed	41-43
Figure 18. Katsumata et al ¹⁸ asymmetry diagnosis boundaries compared to asymmetry diagnosis boundaries using the means and standard deviations from the current study	49

Introduction

Assessing symmetry is important in any esthetic evaluation of the craniofacial region. Many experts consider symmetry to be of high importance in facial attractiveness.^{15,16,30,39} Some researchers have used the chimera technique to compare faces created by mirroring the image of half a face digitally to create a symmetrical face and then comparing it with normal faces.¹⁹ Use of this mirror imaging procedure to evaluate facial attractiveness has given results that have minimized the importance of symmetry,^{20,44} however, these studies use of strict mirroring can cause artificial structural abnormalities that create faces that are abnormal in appearance.³⁸ A potentially better way to assess the importance of symmetry is by mirroring select landmarks on both sides of the face and comparing this new face to the original. In these types of studies, the new symmetrical face is found to be more attractive than the original in studies of both male and female faces.^{38,39}

Facial esthetics is becoming more important in modern society. With this increasing concern for esthetics, orthodontic patients complain of even slight asymmetries. Some patients even believe that asymmetry develops or progresses due to orthodontic treatment.¹⁶ Due to the importance of symmetry in facial esthetics, and the high value patients place on symmetry, asymmetry assessment is an essential component of a successful orthodontic practice.

The purpose of this study is to assess skeletal asymmetry of orthodontic patients using cone beam computed tomography and compare symmetry between patients who are skeletally class II versus those who are skeletally class I. It is hypothesized that

patients with a skeletal class II growth may also have increased levels of skeletal asymmetry in the maxilla and mandible as well as in other regions of the head. This study will utilize an asymmetry index developed by Katsumata et al¹⁸ to assess asymmetry at different craniofacial locations and compare patients with varying ANB angles. It will also compare the mean asymmetry index values at each site compared to the values reported in the literature using this technique.

Etiology, Classification, and Treatment of Craniofacial Asymmetry

The etiology of craniofacial asymmetry is multifactorial. According to Bishara et al³ asymmetry can be due to genetic or congenital malformations, environmental factors, or functional deviations. Congenital malformations that contribute to asymmetry include such conditions as hemifacial microsomia, cleft lip and/or palate, and craniosynostosis as well as a myriad of other syndromes. Examples of environmental factors include pathology, trauma, and wound healing as well as myofunctional habits. Functional deviations create asymmetry from mandibular shifts as a result of functional interferences. Craniofacial asymmetry can exist as dentoalveolar, skeletal, or overlying soft tissue asymmetry or be a combination of these factors.³

Minor asymmetry is typical in most human faces. The point at which “normal” asymmetry becomes “abnormal” is often defined by the individual patient as well as the particular orthodontic clinician’s sense of facial balance.³ Once the asymmetry is classified as abnormal by either the patient or the orthodontist a plan can be created to address the asymmetry. Orthodontics alone can often treat true dental asymmetries, such

as a congenitally missing tooth, as well as functional asymmetries due to occlusal interference.³ Skeletal asymmetries are difficult to resolve solely with orthodontics and can require growth modification or surgery to improve or correct the imbalance.⁴⁵ It is critical to distinguish the location of an asymmetry so treatment can focus on correcting the discrepancy, rather than leaving the patient with a potentially unsatisfactory outcome.¹⁵

Skeletal Asymmetry Relationship to Malocclusion

There are many articles that posit a relationship between dental malocclusion and cranial skeletal asymmetry.^{1,31,36,37,51} Vazquez et al⁵¹ found asymmetry in the majority of the skulls they studied and also found a statistically significant correlation of the asymmetry with the presence of severe dental malocclusion. One relationship between malocclusion and asymmetry cited in the literature is the class II subdivision patient. Janson et al¹⁷ found that a class II subdivision patient has the maxillary midline on with the face and the mandibular midline off towards the class II side 61 % of the time, the mandibular midline on with the face and the maxillary midline off 18 % of the time, and a combination of the two is present 20 % of the time. Alavi et al¹ compared two groups of 28 subjects, one group possessing class II subdivision malocclusions and the other group having normal occlusions. They compared various linear measurements on posteroanterior and lateral cephalometric radiographs as well as dental models between the two groups. They found significant differences between the groups primarily ascribing asymmetrical differences to the mandible in class II subdivision patients. Rose

et al⁴² compared class II subdivision patients to a class I patient group by measuring submentovertex radiographs. They found that the mandibles did not vary in symmetry but that the molar positions did, with the subdivision side mandibular molars being located more posteriorly in these patients.

Another type of malocclusion explored in the literature for its relationship to skeletal asymmetry is posterior crossbite. Studies have documented that children with unilateral crossbite have condyles that are asymmetrically located in the glenoid fossa^{12,22} and that if these crossbites are untreated it can result in asymmetries in condylar length and position with lateral displacement of the ipsilateral condyle³⁷ and increased length of the contralateral condyle.⁴⁶

The present study is taking a different approach by attempting to verify a relationship between asymmetry and a class II skeletal pattern as a whole, diagnosed by ANB angle. It is hypothesized that patients who have an anterior-posterior proportional discrepancy between their upper and lower jaws, such as a class II skeletal patient, may also have a higher proportion of skeletal asymmetry compared to patients with normal jaw proportions.

Radiographic Asymmetry Assessment

Prior to the creation of computed tomographic (CT) imaging, radiographic assessment of asymmetry relied solely upon two dimensional imaging techniques. There are many problems with converting a three-dimensional object such as a human skull into a two-dimensional image. Magnification varies between different regions, with areas

closer to the film magnified less than those nearer the source.⁴⁸ Two-dimensional radiographs are also dependant on head position when investigating asymmetry. Cook⁷ found that a posteroanterior cephalometric radiograph with patient head rotation of five degrees can cause the apparent side of an asymmetry to switch. Another problem is that two-dimensional radiographs are often plagued by bilateral structural superimposition which makes accurate asymmetry assessment difficult.^{4,43} Together, these issues make assessing skeletal asymmetry using two-dimensional radiographs problematic.

Three-dimensional CT images, on the other hand, use a built-in reconstruction algorithm to correct known distortions due to projection geometry,⁵ and allow clinicians to assess skull anatomy either through three-dimensional reconstruction or through accurate two dimensional slices through the skull in any location.

The first CT scanner was invented in 1972 by Godfrey Hounsfield¹⁴, since then these machines have gained greater sophistication and are being utilized in a wider array of clinical applications. In the modern medical CT, the x-ray source rotates within the gantry chamber that houses the x-ray tube and detector, while the patient is moved through the gantry on the bed. This method of CT scanning is known as helical CT and is the most widely used.¹⁴

Although exceptional for three-dimensional imaging, the medical CT places a high economic and biological burden on the patient because of its high cost and high radiation exposure. The recent creation of cone-beam computed tomography specially designed to image the maxillofacial region allows for three-dimensional imaging similar to the medical CT but has the substantial advantages of significantly reduced radiation

and cost. The CBCT uses a single 360 degree rotation of the x-ray tube around the head to acquire the image instead of several rotations in conventional medical CT. This effectively reduces the exposure time and also the absorbed radiation dose to the patient.^{9,32,36,49} The newest low radiation CBCT machines allow maxillofacial imaging in a range similar to that of conventional dental radiographic examinations.^{25,29,47} This lower radiation dose allows CBCT technology to become a effective tool during orthodontic diagnosis and treatment planning.

Previous Three-Dimensional Skeletal Asymmetry Analyses

There are multiple methods detailed by previous authors for analyzing craniofacial asymmetry in three dimensions. These methods can be grouped by the type of data they provide into either qualitative or quantitative methods. Tarajima et⁴⁸ al used wire mesh models of the average man and woman made from CT scans of a group of Japanese men and women with normal faces and occlusions, and compared them to patients to assess asymmetry. This method yields qualitative data about asymmetry location and severity obtained from observing where the patient's own CT anatomy differs from the wire mesh model. By examining the superimposed images, a clinician can ascertain where a deviation is and give an estimated degree of the severity but cannot give a numerical value for the severity that can be compared between patients. This type of qualitative data is what would be expected from other superimposition methods to ascertain three-dimensional asymmetry.

On the other hand, quantitative methods provide information about the location of an asymmetry as well as numerical values of severity. A study by Hyeon-Shik Hwang et al¹⁵ used three dimensional reconstructions of the maxilla and the mandible to make direct measurements to assess asymmetry. They compared maxillary height, ramus length, frontal ramal inclination, lateral ramal inclination, body length, and body height for left and right sides of the structures. This method gives indications of asymmetry within a certain facial bone by itself, but will not assess asymmetry compared to other structures of the skull. A study by Sun-Hyung Park et al³³ investigated asymmetry by setting up three-dimensional reference planes and using a coordinate system to measure various linear distances and angles. They used 30 students with normal occlusion and a balanced face to create normal values which they can then compare to patients to assess asymmetry. This style of analysis will give indications of asymmetry relative to the three-dimensional reference planes. Their study differs from the methods used in the current study in that they examined the linear measures and angles alone for each landmark but did not combine them into an asymmetry index.

The 2005 article by Katsumata et al¹⁸ examined craniofacial asymmetry using a coordinate system based off of reference planes and included an asymmetry index to compare right and left sides of the skull. Their system used the landmarks sella, nasion, and dent (the most superior point of the dens on the axis) to set up the saggital reference plane, the landmarks sella and nasion to set up the axial plane perpendicular to the saggital plane, and the landmark dent to set up the coronal plane perpendicular to the other two planes. They then identified landmarks on 16 patients who were determined by

a panel of 3 radiologists to have no craniofacial asymmetry in the hard tissues. The coordinates of various landmarks were inserted into an asymmetry index calculation that summed the differences in location from a bilateral landmark to the reference planes and takes the square root of the summation. This is the equation they used:

$$AI = \sqrt{(Rdx - Ldx)^2 + (Rdy - Ldy)^2 + (Rdz - Ldz)^2}$$
 where R=right and L=left and dx,

dy, and dz are the distances to the various facial planes. They averaged the asymmetry index values for 12 landmarks of the 16 patients to create normal values that can be compared to other patients to assess asymmetry at the landmark locations. Their method forms the basis for the asymmetry index calculations of the present study.

Landmark Identification with CBCT

There are unique difficulties with identifying landmarks on three-dimensional CBCT images compared to identification on a lateral cephalometric film. Most cephalometric landmarks do not have well accepted operational definitions in all three planes of space.⁹ Some landmarks can be easily identified in one or two planes of space, but identification in the third plane of space can be difficult. In these cases observers tend to locate the landmarks in the planes of easiest visualization.^{9,26} Difficulty is created by inclusion of the medio-lateral dimension to landmark location, a dimension which was not considered when lateral cephalometric landmarks were created.²⁶ Some two-dimensional cephalometric landmarks are constructed from overlapping structures, such as articulare, which makes them unsuitable for three-dimensional imaging. A final challenge to landmark identification is that many landmarks require identification of the

centroid of a specific three-dimensional structure. These landmarks are known as fuzzy landmarks.^{21,50} The best three-dimensional landmarks are those that are easily located in three planes of space and are biological or sharply delineated. New landmarks that take this into account will be greatly beneficial.^{9,23,24}

Some authors have identified specific landmarks that are difficult to localize on a three-dimensional image. A person with a flat mediolateral orbital form presents a challenge for localizing orbitale in the axial plane. A saddle shaped or flat condyle can make identifying condylion more challenging. Porion can be difficult to localize in both mediolateral and cranio-caudal dimensions.²⁶ In contrast to these landmarks, one study demonstrated that ANS, which is a sharp anatomical point, may be more easily identified using a CT image compared to a conventional lateral cephalogram.²¹

Even though there are some difficulties with identifying landmarks on CBCT films, there are also some advantages. A lack of superimposed structures creates easier visualization of certain skull regions, and CT images are not plagued by geometric distortion.^{4,6,43}

Another advantage to CBCT landmark identification is visualization using the stacks of CT slices, or the multiplanar reconstruction (MPR) images. This allows inspection from any of the three planes of space to help identify landmarks from multiple views. An article by Grauer et al¹⁰ recommends identifying landmarks on the MPR images rather than on the three-dimensional rendered image. Their reason is that the rendered image is dependent on many factors such as image contrast, movement during

acquisition, signal-to-noise ratio of the image, and threshold filters applied by the operator.

Various studies have investigated the accuracy of landmark localization on CBCT images. Many have found the process both accurate and reproducible. Oliveira et al⁹ found that three-dimensional landmark identification using CBCT can offer consistent and reproducible data if a protocol for operator training and calibration is followed. In their study, intra- and inter- observer differences in landmark location were quite small. Ludlow et al²⁶ compared landmark identification on the MPR images created by CBCT to lateral cephalometric landmark identification and found that landmark identification was accomplished with statistically significantly less variability on MPR views. Richtsmeier et al⁴¹ identified 35 skeletal landmarks in three-dimensions and found average error of less than 0.5mm for all landmarks and less than 0.2mm for 13 of the 35. A study by Kragstov et al²¹ found variations of less than 1mm for landmarks identified on lateral cephalograms compared to variations of up to 2mm on helical CT images. A study by Valeri et al⁵⁰ demonstrated average error of 1.15mm in localization of fuzzy landmarks. They concluded that such landmarks are usable in research.

Linear Measurement Accuracy with CBCT

When assessing asymmetry using CBCT images and attempting to obtain quantitative data, it is necessary to make multiple linear measurements. Therefore, it is important that linear measurements are accurate and reproducible using CBCT technology, and various authors have executed studies that assess this. Overall, these

studies support the accuracy and reproducibility of linear measurements on CBCT. A study by Hilgers et al¹³ measured linear distances between 11 anatomic sites using digital calipers and on CBCT images obtained using an iCAT (Imaging Sciences International, Hatfield, PA) CBCT machine. They found that in all instances, the CBCT obtained measurements were highly accurate and intraobserver reliability was good. This is relevant to the present study which will also use images obtained from an iCAT CBCT machine. Ludlow et al²⁷ also found that three-dimensional measurements of anatomy using CBCT are acceptably accurate. Williams et al⁵² measured 378 linear distances using spiral CT images of dry skull mandibles and compared the measures to those made using a table-top digitizer. They found a mean error of 0.377mm. Richtsmeier et al⁴¹ also investigated linear measures using a spiral CT and found differences of 1-2mm in measures made directly using a table-top digitizer compared to measures on the CT images. A CBCT linear measurement study by Berco et al² found errors of approximately 0.2mm in the three planes of space and no errors greater than the voxel size of the scans of 0.4mm. Pinsky et al³⁵ measured an acrylic block on a dry skull mandible using digital calipers and CBCT and found mean differences of less than 0.04mm for the block and less than 0.28mm for the mandible, using a scan with a voxel size of 0.2mm. Another study made twenty linear measurements on 23 dry skulls using digital calipers and CBCT and found that 40 percent of the measurements had less than 1mm difference, 70 percent had less than 1.5mm difference, and 90 percent had less than 2mm difference between the two measurement modalities.³⁴

There are several variables that could influence accuracy of linear measurements reported in the literature. Voxel size, type of image detector, scanning time, reconstruction time, radiation dose, and head position have all been mentioned as variables that could affect CBCT linear measurements.^{2,9} For these reasons, it is possible that there are significant differences in accuracy and reliability from one CBCT machine to another. One study scanned dry skulls in incrementally rotated malpositions using CBCT and found that measurement was not significantly influenced by variation in skull orientation.²⁷ Another study by Hassan et al¹¹ confirmed that head position is not important in CBCT measurement accuracy on hard tissues. The effect of voxel size on CBCT linear measurements was investigated by Damstra et al.⁸ They compared CBCT measurements using 0.4mm and 0.25mm voxel sizes and compared to digital caliper measurements on dry mandibles. They reported high accuracy using either voxel settings with no difference in accuracy between the two groups.

Aim

To determine if there is a difference in skeletal asymmetry between patients with a class I ANB angle compared to patients who have a class II ANB angle based on the assessment method developed by Katsumata et al.¹⁸ It is hypothesized that patients with a skeletal class II growth pattern may also have increased levels of skeletal asymmetry.

Objectives

- 1) To check for a relationship between ANB angle and skeletal asymmetry. ANB will be examined both as a continuous variable and also by grouping patients into class I versus class II ANB angles.
- 2) Compare the means and standard deviations of asymmetry index values for landmarks of patients in this study compared to the means and standard deviations cited in the Katsumata article.¹⁸
- 3) Assess reliability of the method through repeat analysis of a portion of the patients.

Null Hypothesis

- 1) There is no relationship between skeletal asymmetry and ANB angle when patients are grouped into class I or class II ANB angles.
- 2) There is no relationship between skeletal asymmetry and ANB angle when ANB angle is investigated as a continuous variable.

Materials and Methods

This study examined CBCT radiographs of 70 patients that were obtained as part of diagnostic record gathering for comprehensive orthodontic treatment at the University of Minnesota. The patients were consecutively selected and fit inclusion and exclusion criteria. Patients were included starting from the first CBCT scans for routine care in July of 2008 until each patient group was filled. This included CBCT scans up to July 2009. ANB angles were measured on orthogonal lateral cephalometric headfilms extracted from the CBCT radiographs and digitized and measured using Dolphin 11.5 betabuild 15 (Dolphin Imaging and Management Solutions, Chatsworth, CA). ANB angles were verified by redigitizing A point, B point, and Nasion landmarks on the radiograph if the initial angle was within 1 degree of a group boundary. One group of thirty patients had ANB angles ranging from -0.5 degrees to 3.4 degrees, this was designated the class I group. A second group of thirty patients had ANB angles of 4.5 or higher, this was designated the class II group. A third group of 10 patients were selected that had ANB angles between 3.4 and 4.4 degrees to enable examination of ANB as a continuous variable. Patients were included who were in the age range from 11 years 0 months to age 15 years 11 months who had CBCT films and fit into a required ANB group angle. Patients were excluded who had been marked during clinical examination or through examination of the photographs to have a CR/CO shift, a posterior crossbite, a first molar in dental crossbite, a lack of a first molar, or a craniofacial anomaly or

syndrome including cleft lip or cleft palate. The class I group had a mean ANB angle of 1.7 degrees with a standard deviation of 1.2 degrees and a range from -0.5 to 3.4 degrees. The mean age for this group was 13 years 3 months with a standard deviation of 1 year 1 month and a range from 11 years 2 months to 15 years 1 month. The class II group had a mean ANB angle of 6.3 degrees with a standard deviation of 1.4 degrees and a range from 4.6 to 10.2 degrees. The mean age for this group was 13 years 3 months with a standard deviation of 1 year 3 months and a range from 11 years 5 months to 15 years 11 months. The group of ten patients had a mean ANB angle of 4.0 degrees with a standard deviation of 0.3 degrees and a range from 3.5 to 4.4 degrees. The mean age for this group was 13 years 4 months with a standard deviation of 1 year 1 month and a range from 11 years 9 months to 15 years 1 month.

CBCT images were acquired with a Next Generation iCAT CBCT unit (Imaging Sciences International, Hatfield, PA). The device was set for 18.54 mAs and 120 kV. The scan was made with a single 360 degree rotation, 8.9 second scan and created images with a voxel size of 0.3mm. The head was oriented by adjusting the chin support until the midsagittal plane was perpendicular to the floor. Patients were biting in centric occlusion during image exposure. Lateral scout radiographs were taken and small adjustments were made to ensure inclusion of all areas of interest and to minimize head orientation errors. DICOM files obtained from the CBCT scan were reconstructed by Dolphin 3D, which is part of Dolphin 11.5 (betabuild 15), and all landmark identifications and measurements were made using this software. Images were visualized

on a Dell 1908FP monitor (Dell Inc., Round Rock, TX) with a resolution of 1280X1024 at 60 Hz.

Asymmetry assessment for this study was conducted in a manner similar to the study by Katsumata et al.¹⁸ Craniometric landmarks were identified as defined in table 1, using the definitions included in a follow up study to the original by Katsumata et al.²⁸ Figures 1-14 demonstrate the MPR slices and three-dimensional reconstructions used to locate each landmark. All landmarks in this study were identified by the primary author. This study strove to utilize whichever views were most advantageous for landmark localization of each individual landmark. The views varied from landmark to landmark, but were constant between subjects. For most landmarks, identification was limited to MPR images only. In identifying orbitale, the three-dimensional reconstruction view was used as it allowed better medio-lateral localization than the MPR images (figure 8). In identifying gonion, the three-dimensional reconstruction was used as it gave a broad picture of the ramus and body and thus made anterior-posterior and superior-inferior identification more accurate (figure 14). This study did not include the landmark pterygomaxillary fissure, which was included in the article by Katsumata et al¹⁸, as preliminary investigation demonstrated difficulty in accurate identification.

The landmarks Sella, Nasion, and Dent were used to create the three reference planes which were used to measure linear distances from each of the other landmarks, as demonstrated in figure 15. The mid-sagittal plane was defined as passing through the landmarks Sella, Nasion, and Dent. The axial plane was defined as passing through Sella and Nasion and being perpendicular to the mid-sagittal plane. The coronal plane was

defined as being perpendicular to the other two planes and passing through Dent. Orienting the reference planes to the reference landmarks required careful manual movements of the reference planes in Dolphin 3D. To minimize error due to plane orientation, the reference planes were not accepted until the plane was less than or equal to 0.2mm from the landmarks it was designed to include. For the remaining landmarks, the distances to each plane was calculated by Dolphin 3D in millimeters by orienting the coordinate plane system to the reference planes. This gave a dx, dy, and dz value for that landmark, with dx the distance to the sagittal plane, dy the distance to the axial plane, and dz the distance to the coronal plane. The linear measurements were exported into the Excel spreadsheet application (Microsoft Corporation, Redmond Washington) for analysis.

For solitary landmarks located near the midline, the asymmetry indices (AI) were defined as the distance to the sagittal plane (AI=dx). For bilateral landmarks the asymmetry indices were calculated using the following formula, where R=right, L=left:

$$AI = \sqrt{(Rdx - Ldx)^2 + (Rdy - Ldy)^2 + (Rdz - Ldz)^2}$$

30 patients were randomly selected using the random number generator function of Excel to have landmarks and reference planes re-identified and asymmetry indexes recalculated to test the reproducibility of the method.

Table 1. Landmark definitions for asymmetry assessment		
	Landmark	Definition on CBCT image
Landmarks for the determination of the reference planes	Sella	Center of the pituitary fossa
	Nasion	Nasofrontal suture at the midline
	Dent	The most superior point of the dens on the axis
Landmarks for the evaluation of facial asymmetry (* denotes bilateral landmarks)	ANS	Tip of the anterior nasal spine
	Upper Central Incisors	The crest of the alveolar ridge between the upper central incisors
	Lower Central Incisors	The crest of the alveolar ridge between the lower central incisors
	Menton	The lower border of the mid-mandibular suture
	Orbitale *	The mid-point of the infra-orbital margin
	Porion *	The superior surface of the external auditory meatus
	Upper First Molar *	The center of the pulp cavity at the crown of the upper first molar
	Lower First Molar *	The center of the pulp cavity at the crown of the lower first molar
	Condyle *	The most superior point of the condyle
	Coronoid *	The most superior point of the coronoid process
	Gonion *	The most inferior and posterior point at the angle of the mandible

Figure 1. Sella was identified on saggital, axial, and coronal slices.

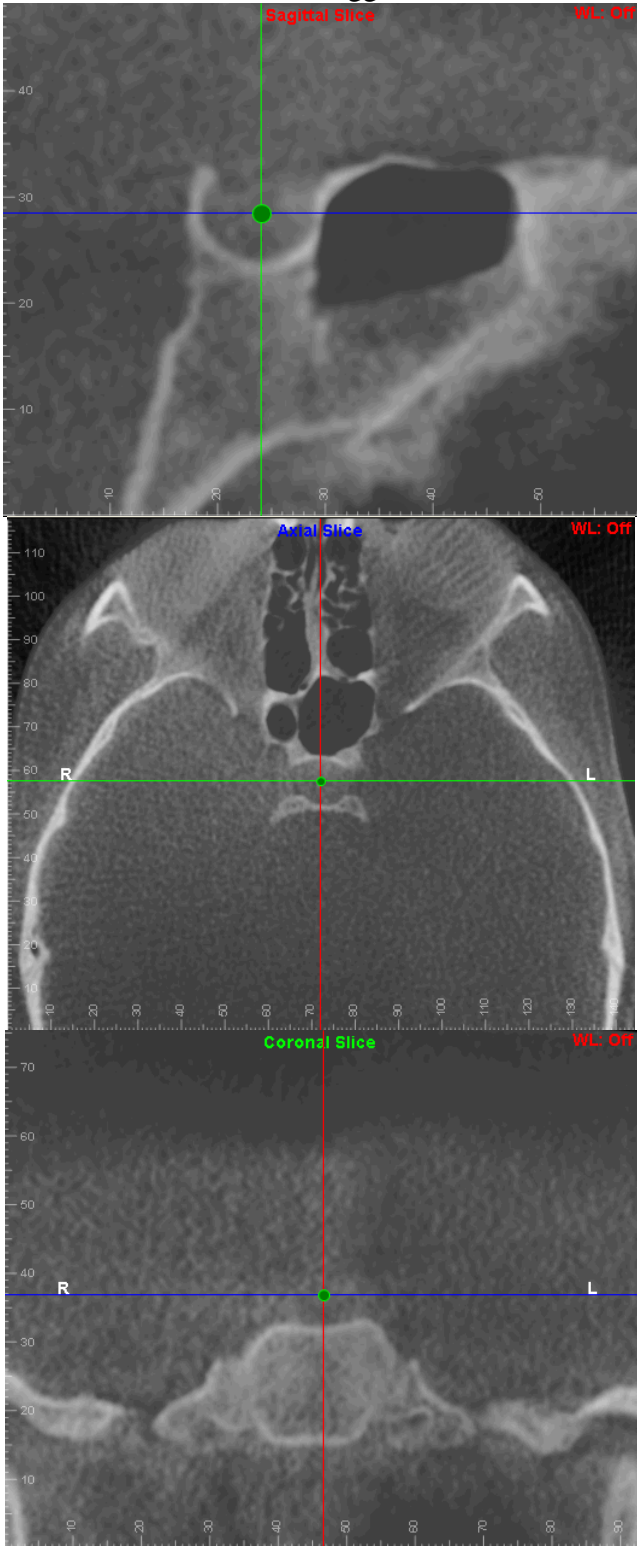


Figure 2. Nasion was identified on saggital, axial, and coronal slices.

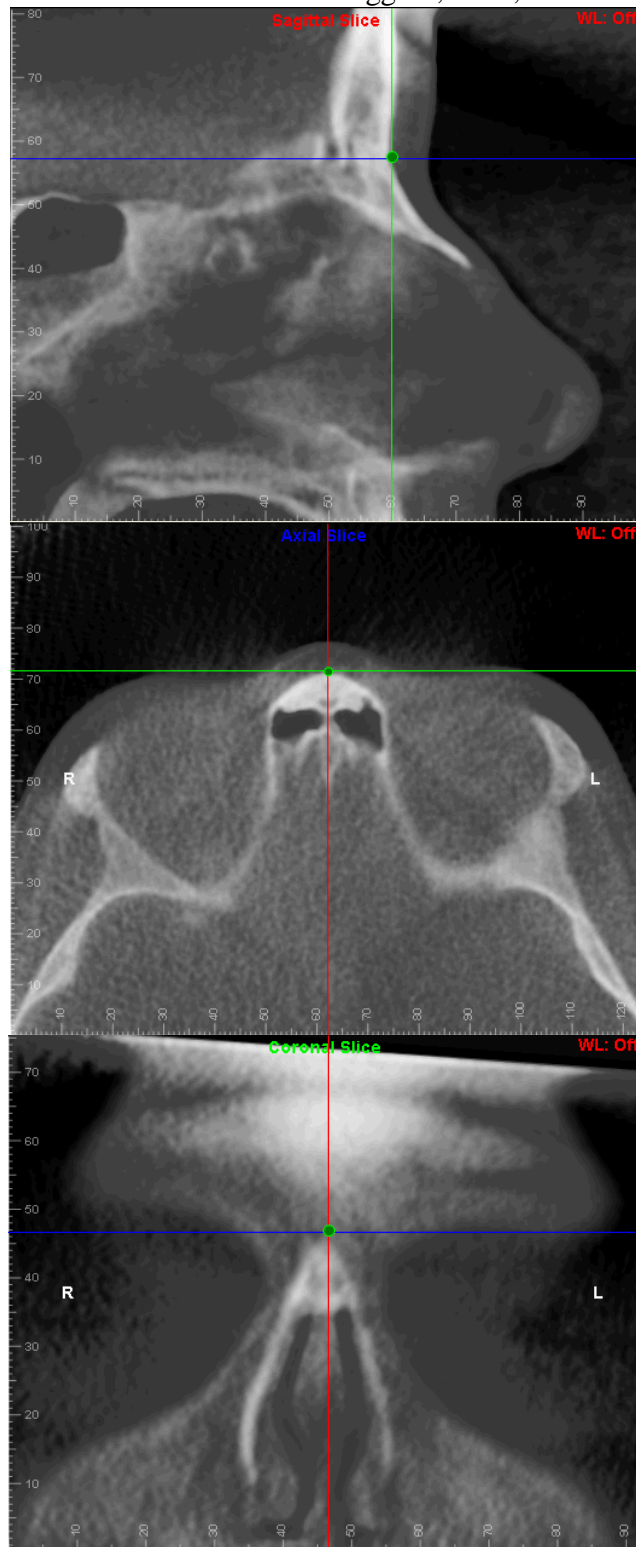


Figure 3. Dent was identified on saggital, axial, and coronal slices.

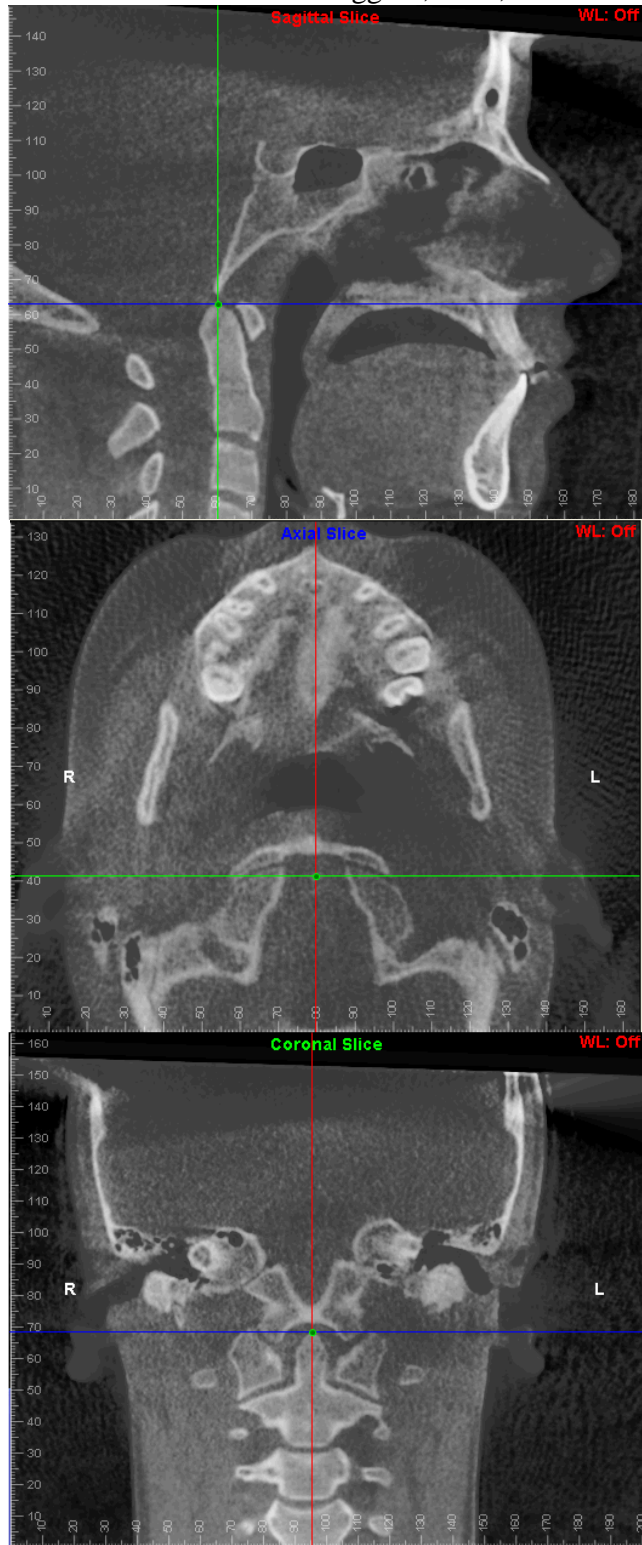


Figure 4. ANS was identified on sagittal and axial slices.

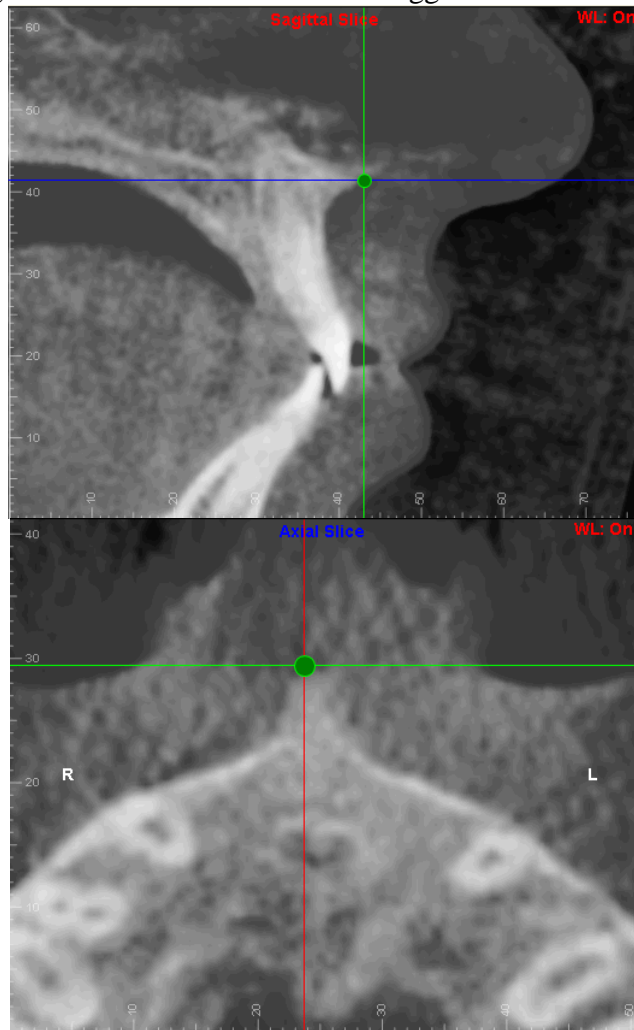


Figure 5. Upper Central Incisors was identified on saggital, axial, and coronal slices.

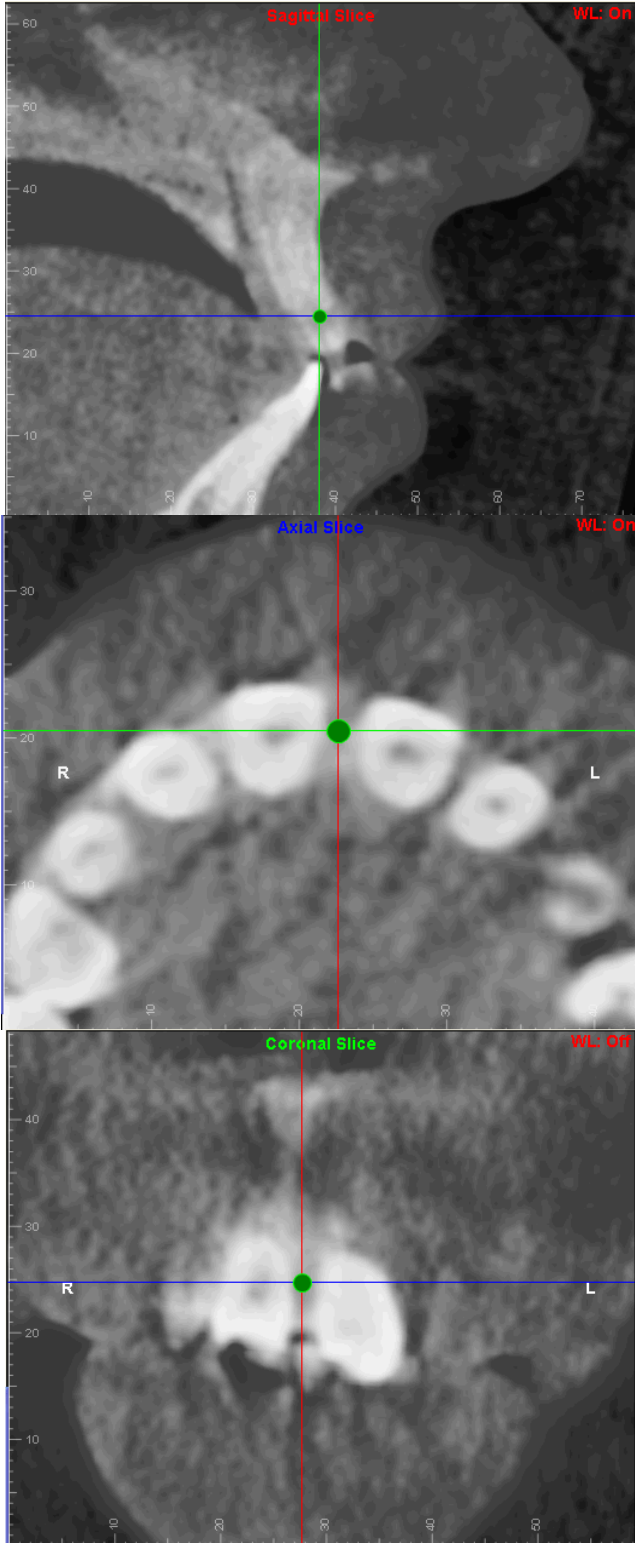


Figure 6. Lower Central Incisors was identified on saggital, axial, and coronal slices.

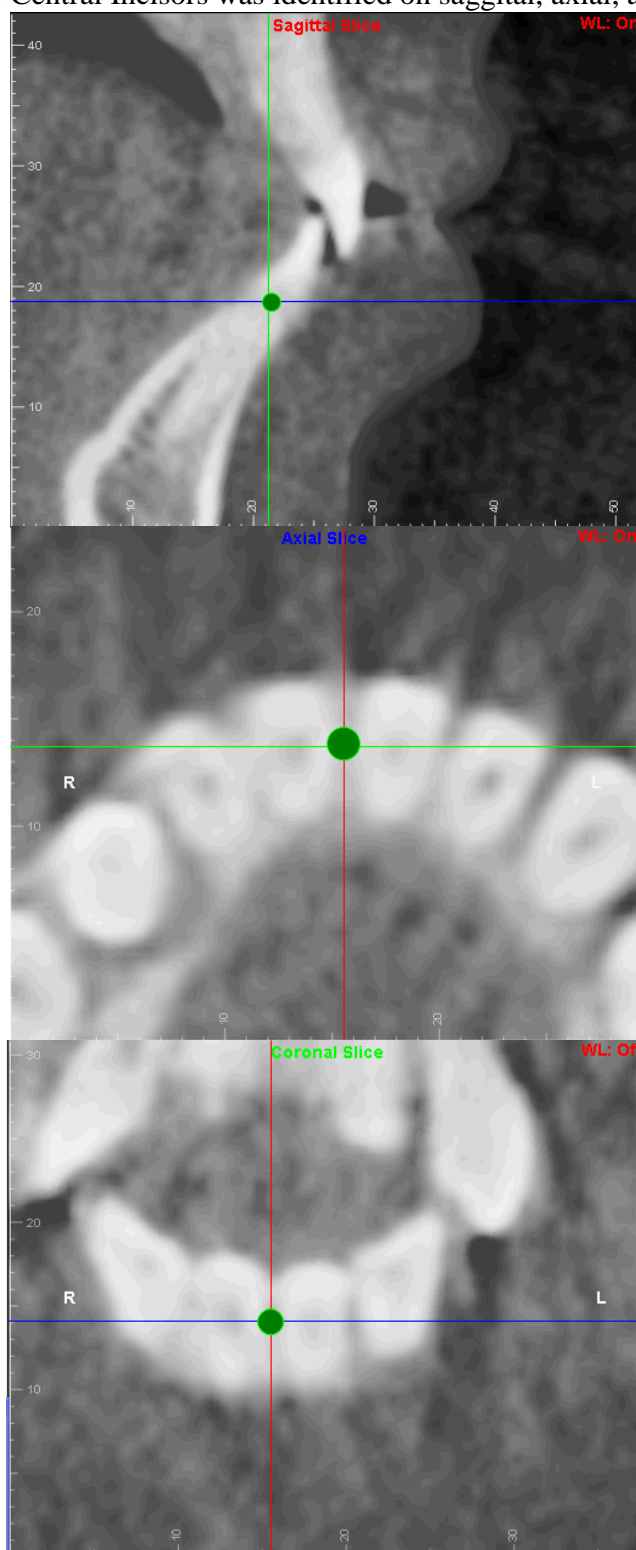


Figure 7. Menton was identified on saggital and coronal slices.

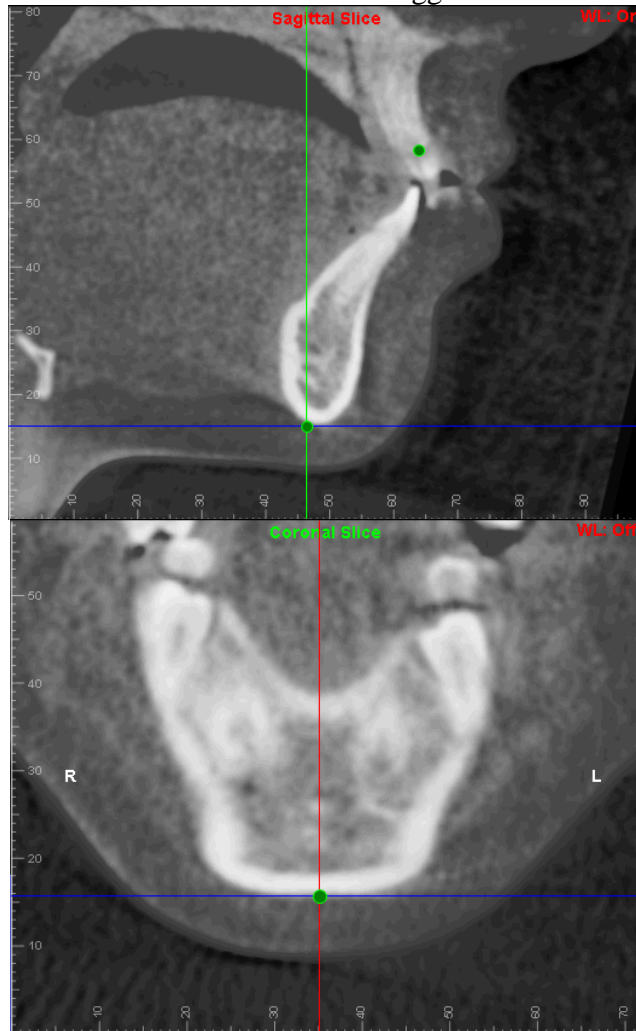


Figure 8. Orbitale was identified on the saggital slice and coronal slice as well as on a three dimensional rendered image viewed from the anterior aspect.

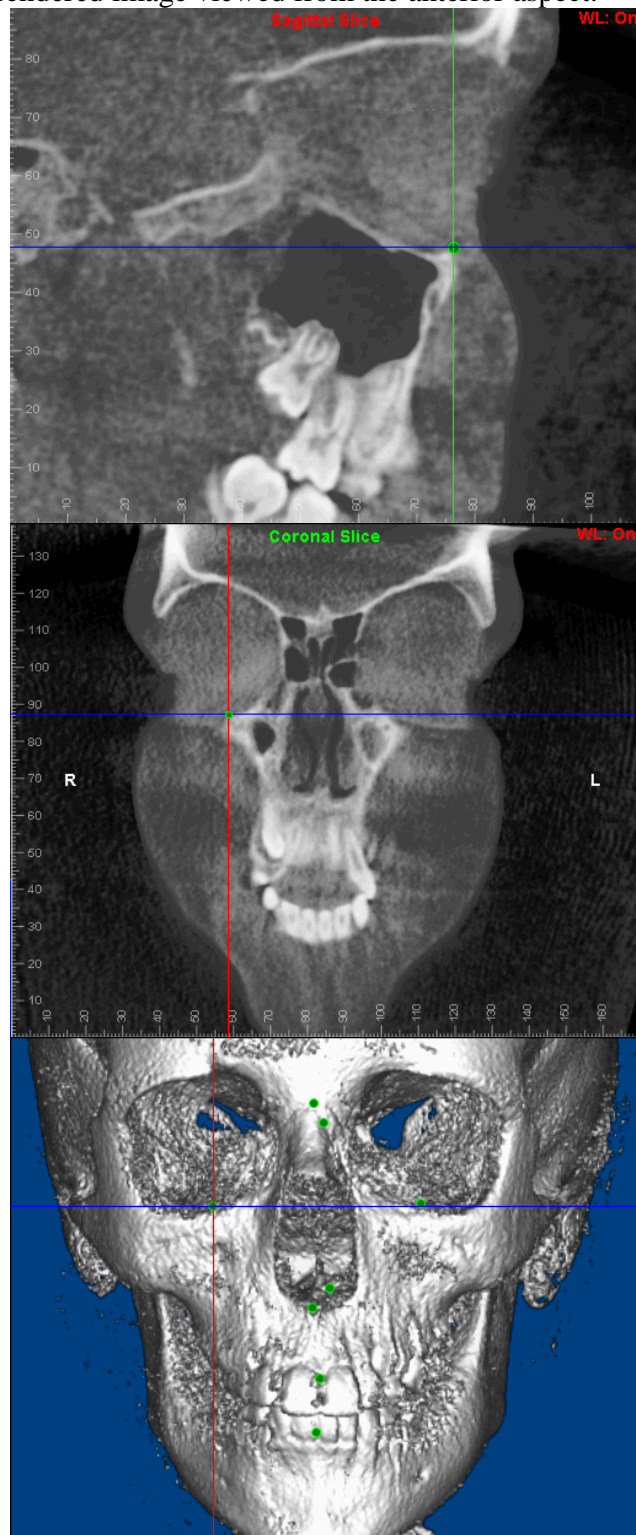


Figure 9. Porion was identified on saggital and coronal slices.

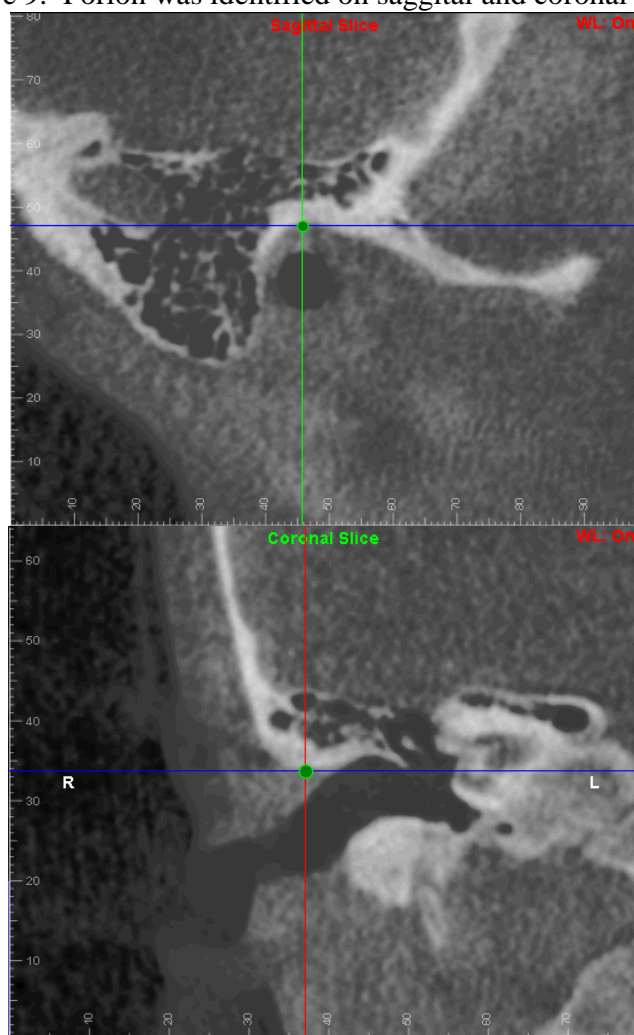


Figure 10. Upper First Molar was identified on saggital, axial, and coronal slices.

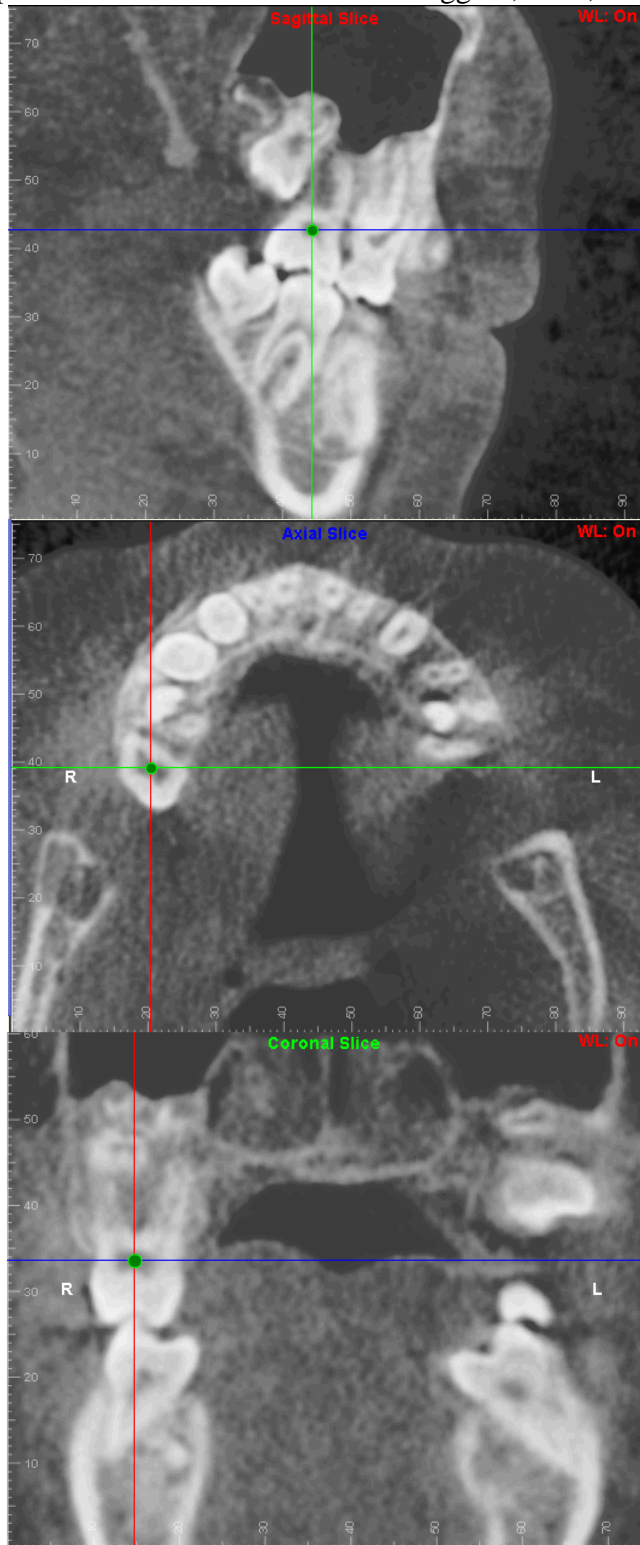


Figure 11. Lower First Molar was identified on saggital, axial, and coronal slices.



Figure 12. Condyle was identified on saggital, axial, and coronal slices.

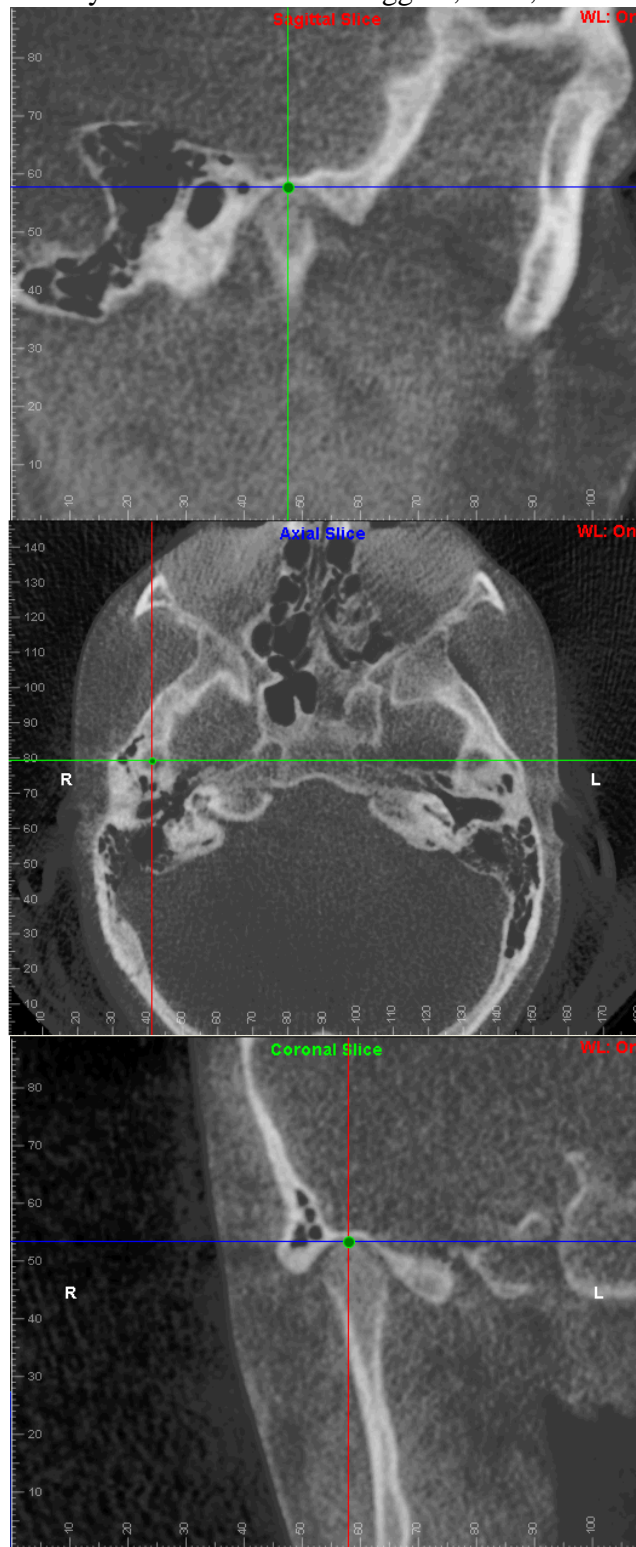


Figure 13. Coronoid was identified on saggital, axial, and coronal slices.

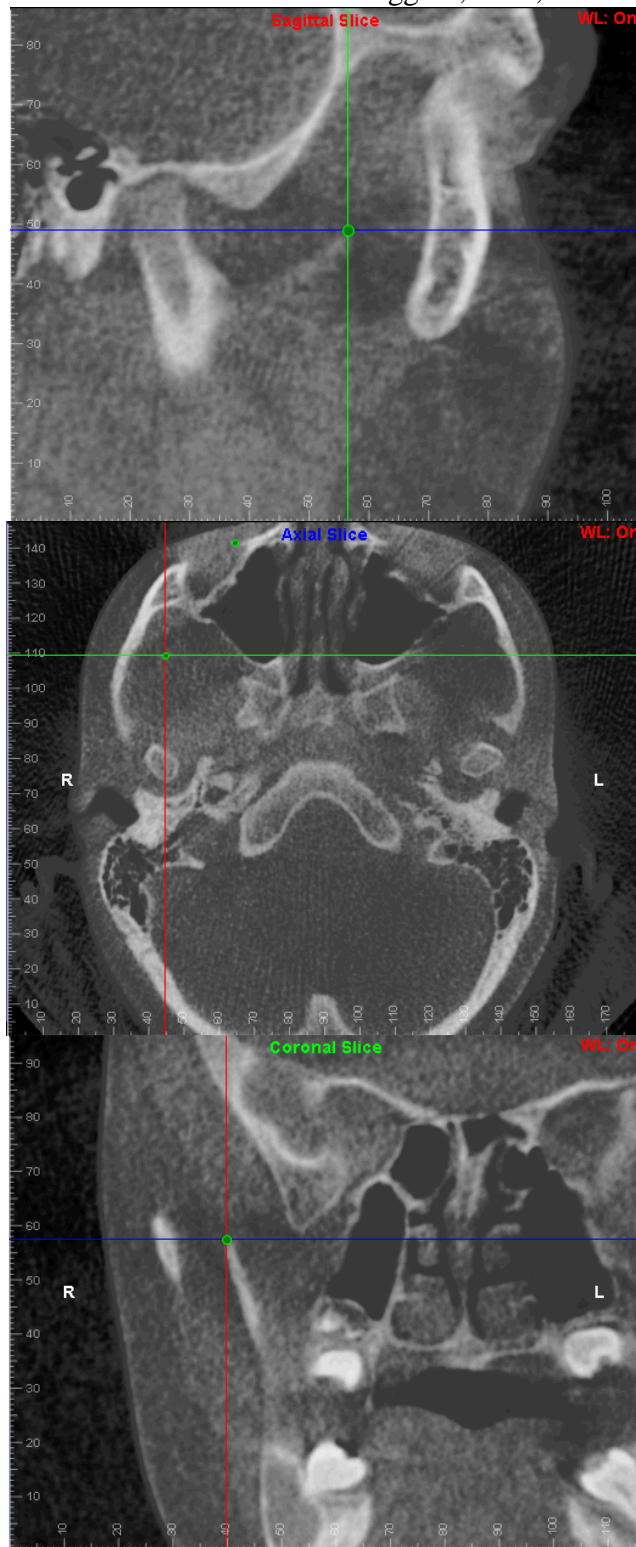


Figure 14. Gonion was identified on sagittal and coronal slices as well as on the three-dimensional rendered image viewed from the lateral aspect.

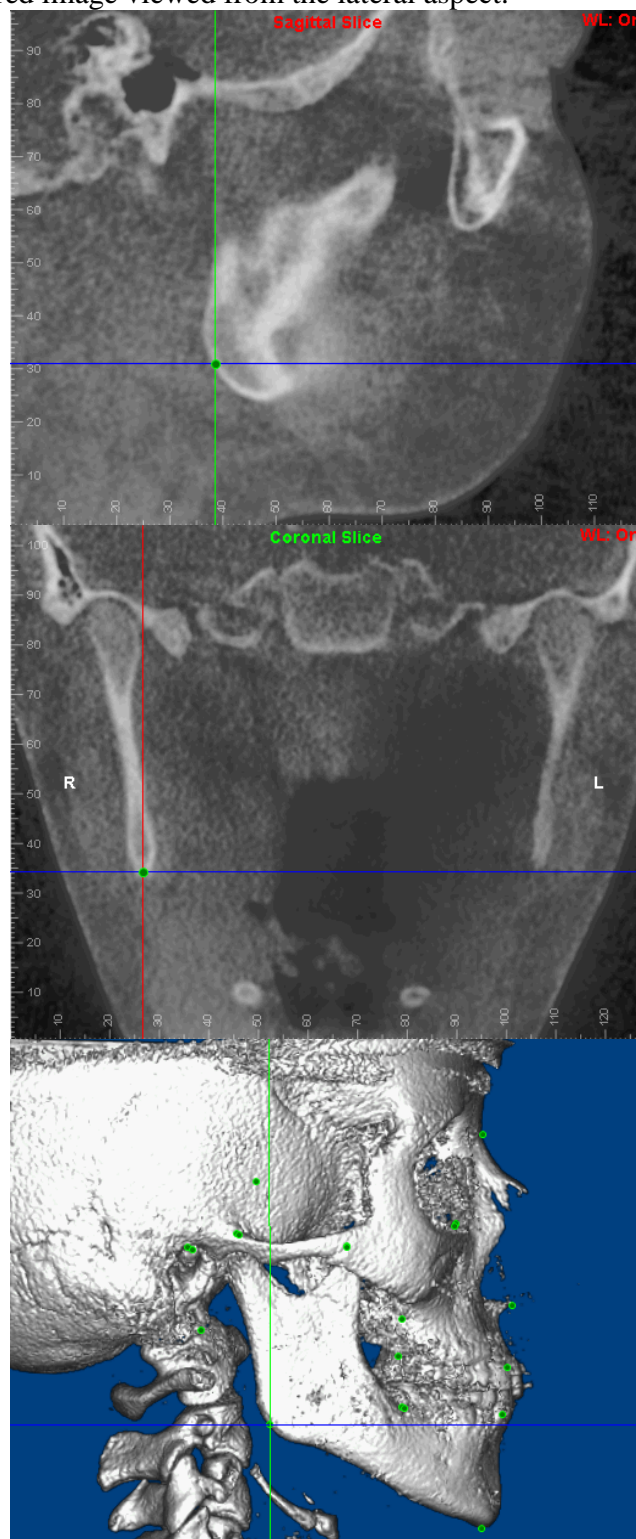
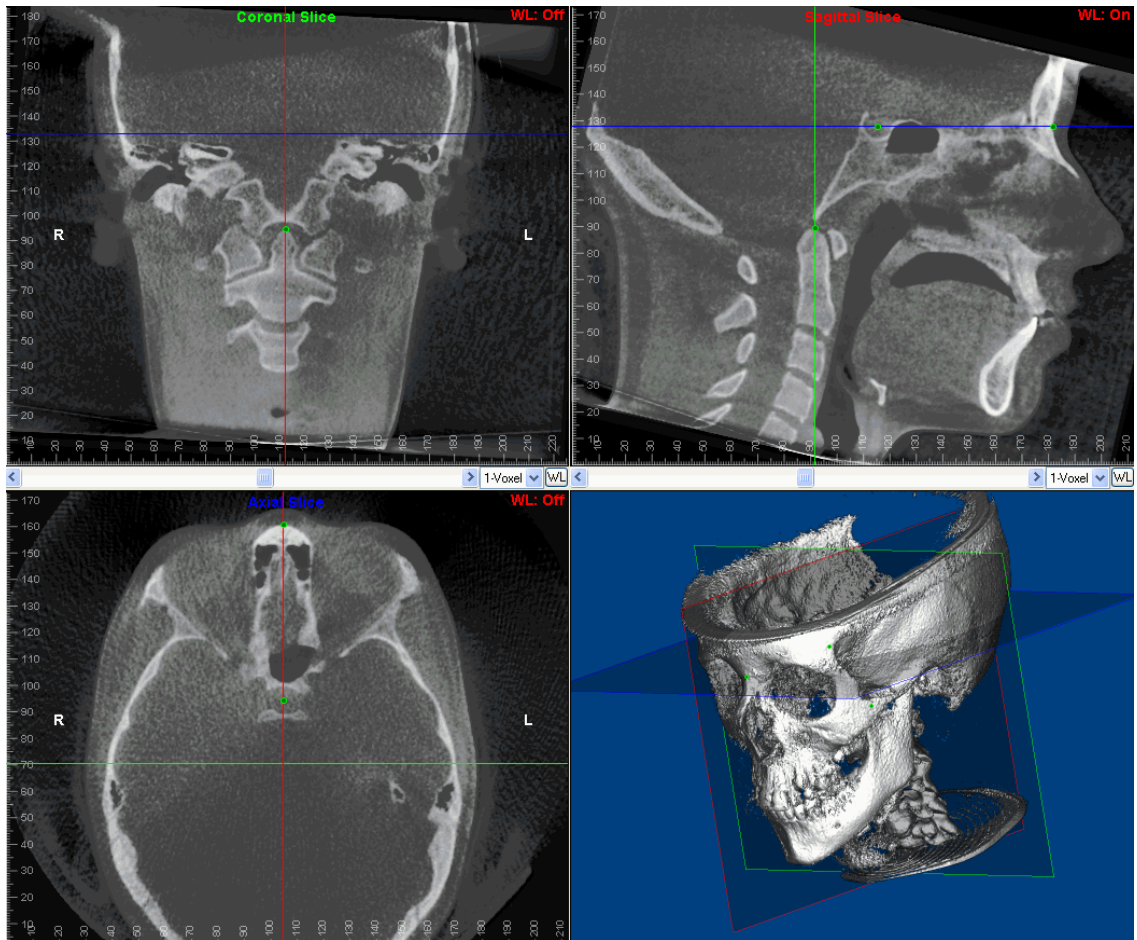


Figure 15. The reference planes used in this study demonstrated on MPR images and three-dimensional reconstruction.



Statistical Analysis

The relationship of skeletal asymmetry and ANB angle as a continuous variable was investigated using Pearson correlation coefficients and scatter plots of the data. The asymmetry index value and corresponding patient ANB angle was analyzed for all patients. Analysis of variance (ANOVA) was performed to compare the three patient groups to see if the mean asymmetry index score was different for any of the landmarks between any of the ANB patient groupings. A two-sample student t-test was performed comparing the mean asymmetry index values and standard deviations found in this study to the values from the previous study by Katsumata et al¹⁸. To assess reliability of measurement Pearson correlation coefficients and Altman-Bland plots compared the original data to the thirty randomly selected patients for re-measure.

Results

Pearson correlation coefficients examining the presence of a linear relationship of ANB to asymmetry index score were calculated for each landmark across all patients and the results are in table 2. None of the coefficients are statistically significant for a linear relationship between ANB and asymmetry index score for any landmark. Scatter plots of the continuous data are shown in figure 16. Visual inspection of the plots gives no apparent support for any non-linear relationships between ANB and asymmetry index score.

ANOVA results compared mean asymmetry index scores for statistically significant differences between any of the three groups of patients grouped by ANB angle. The groups were the patients with ANB angles from -0.5 to 3.4 degrees (30 patients), the patients with ANB angles from 4.5 and higher (30 patients), and the patients with ANB angles between 3.5 and 4.4 degrees (10 patients). Table 3 gives F and P values for each ANOVA test for each landmark. No significant differences in the mean asymmetry index values were found for any landmark.

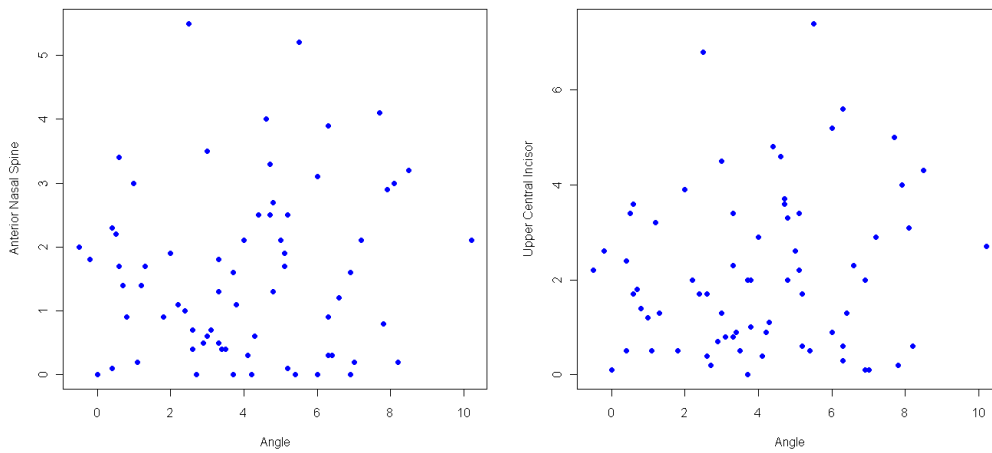
Because there were no significant differences in asymmetry index scores relative to ANB angle, the scores from all groups were combined to find an asymmetry index mean score and standard deviation for each landmark. These were compared with the means and standard deviations found by Katsumata et al¹⁸ in his study and the results were compared by a two sample student t-test. The results are in table 4. All means except for landmarks coronoid process and gonion were significantly different at the $p=0.05$ level and the direction for all was an increase in asymmetry index score.

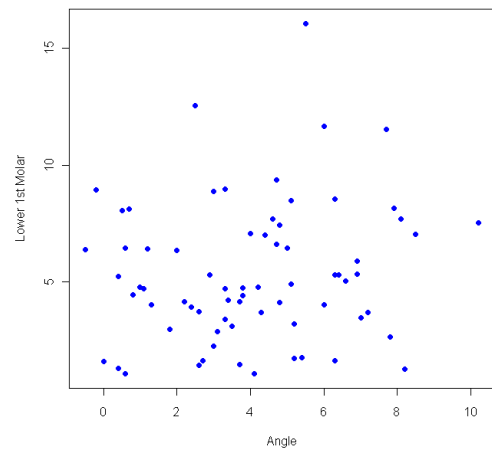
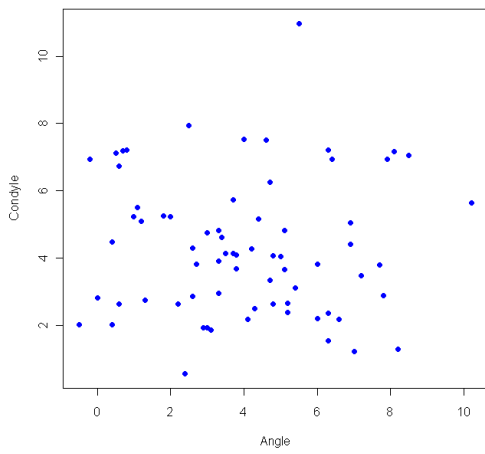
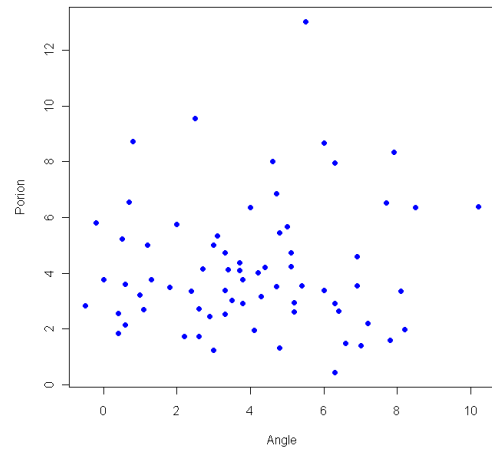
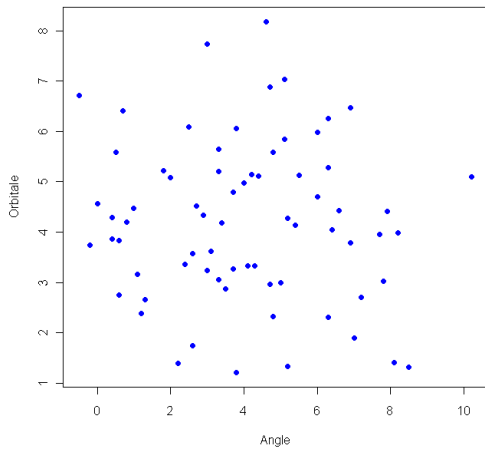
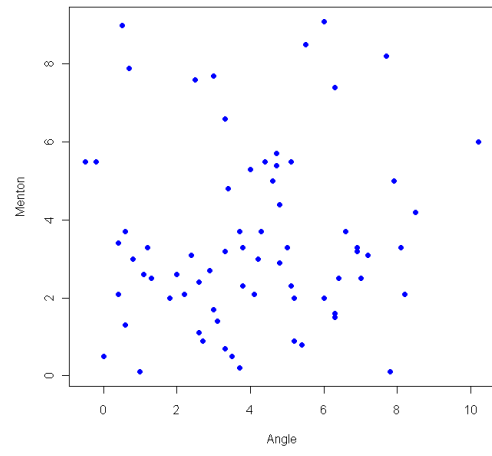
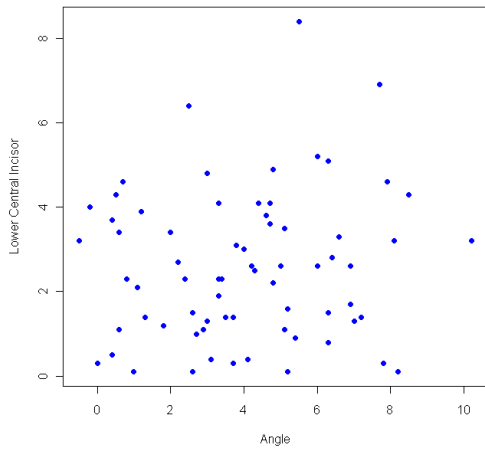
Reproducibility of asymmetry index scores was assessed through repeat measurement of 30 randomly selected patients of the original 70 patients. Pearson correlation coefficients between mean asymmetry index scores and the new scores for each of the landmarks are shown in table 5. All correlations are significant at $p<0.05$ and all but orbitale are significant at $p<0.0001$. Altman-Bland plots were also utilized to compare reproducibility of the asymmetry index scores as they give more information about agreement range and bias of repeated data. A summary of the Altman-Bland Plots

is in table 6 and the plots are shown in figure 17. The summary data demonstrates no bias in direction of agreement as none of the landmarks had a p value less than 0.05.

Table 2. Pearson Correlation Coefficients of ANB and landmarks across all patients.		
<u>Landmark</u>	<u>Correlation Coefficient</u>	<u>P Value</u>
ANS	0.110	0.365
Upper Central Incisors	0.139	0.252
Lower Central Incisors	0.105	0.387
Menton	0.078	0.522
Orbitale	-0.078	0.520
Porion	0.072	0.551
Upper First Molar	0.085	0.483
Lower First Molar	0.143	0.236
Condyle	-0.011	0.927
Coronoid	0.060	0.619
Gonion	0.054	0.660

Figure 16. Scatter plots of the continuous data on 70 patients comparing ANB angle to asymmetry index scores. The ANB angles are on the x-axis and the asymmetry index scores are on the y-axis of the plots.





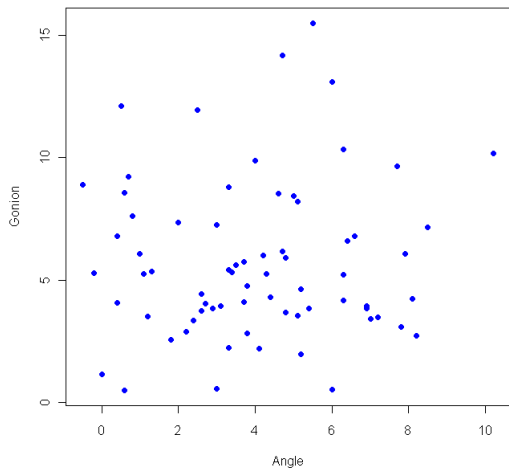
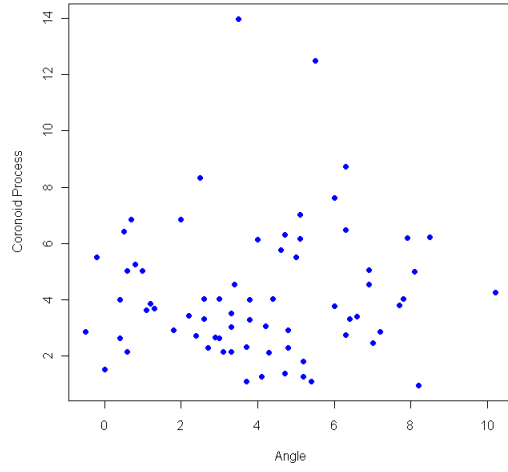
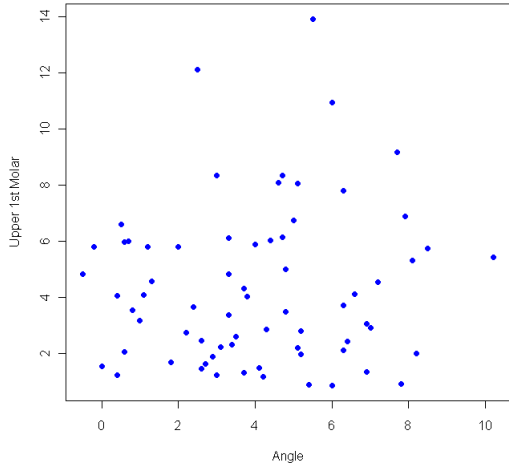


Table 3. ANOVA F and P values comparing mean asymmetry index score for each group at each landmark		
<u>Landmark</u>	<u>F Value</u>	<u>P Value</u>
ANS	2.28	0.110
Upper Central Incisors	1.79	0.179
Lower Central Incisors	1.01	0.369
Menton	0.67	0.514
Orbitale	0.09	0.913
Porion	0.61	0.549
Upper First Molar	1.42	0.250
Lower First Molar	2.13	0.127
Condyle	0.03	0.974
Coronoid	0.49	0.616
Gonion	0.85	0.430

Table 4. Comparing mean asymmetry index scores from the present study and previous study by Katsumata et al. ¹⁸ *denotes significant difference at p=0.05 level					
Landmark	Katsumata ¹⁸		Current		P-Value
	mean asymmetry index values	Katsumata ¹⁸ standard deviation	study mean asymmetry index values	study standard deviation	
ANS	0.8	0.7	1.6	1.3	0.002 *
Upper Central Incisors	0.9	0.8	2.2	1.7	<0.0001 *
Lower Central Incisors	1.2	1.2	2.6	1.7	0.0006 *
Menton	1.8	1.1	3.5	2.3	<0.0001 *
Orbitale	1.7	0.8	4.2	1.6	<0.0001 *
Porion	2.7	1.0	4.2	2.3	0.0002 *
Upper First Molar	3.1	1.0	4.3	2.8	0.004 *
Lower First Molar	2.9	1.4	4.3	2.0	0.002 *
Condyle	3.2	1.4	5.4	3.0	<0.0001 *
Coronoid	3.7	1.3	4.2	2.4	0.256
Gonion	4.6	1.7	5.7	3.2	0.052

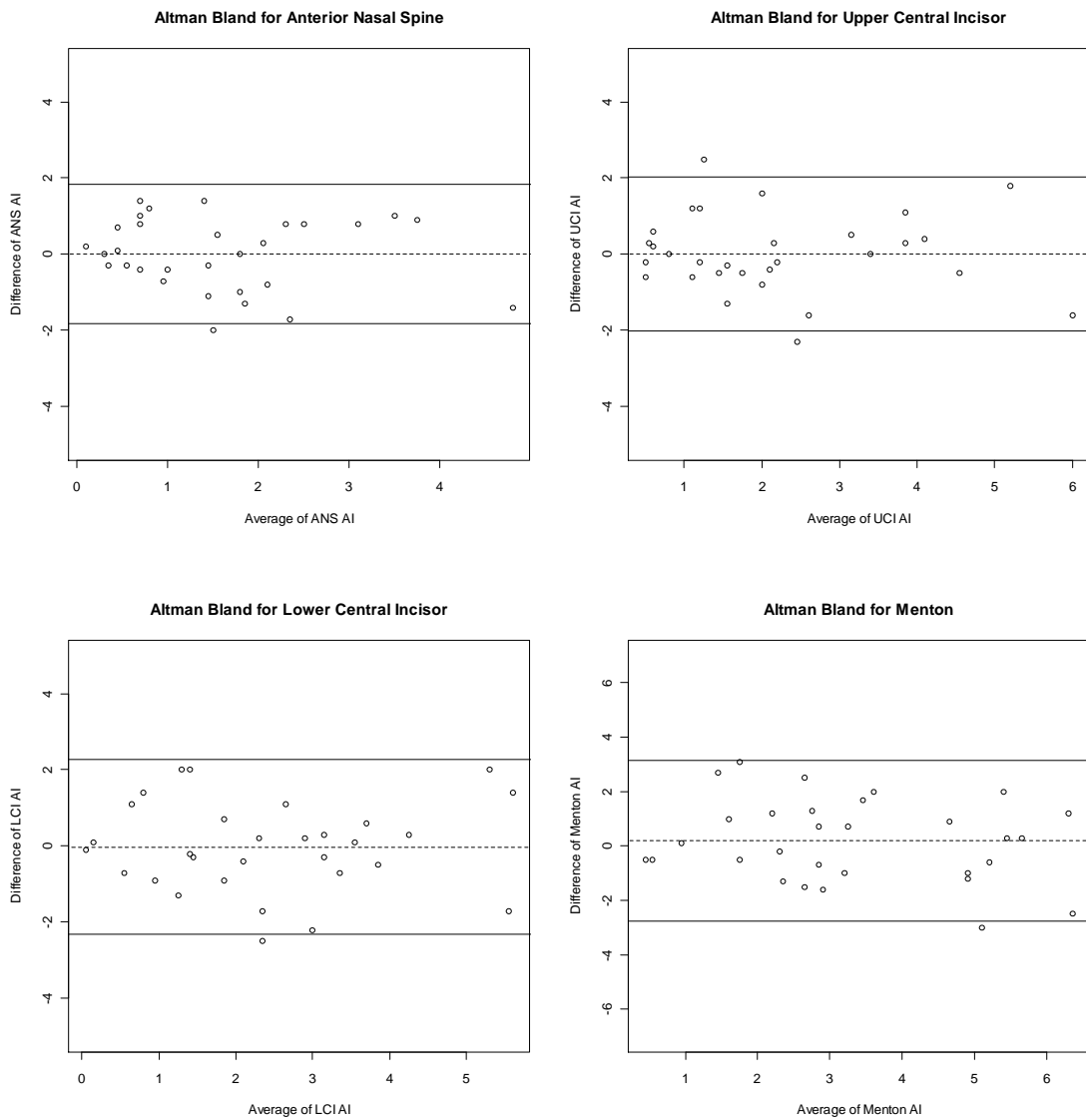
Table 5. Pearson correlation coefficients comparing mean asymmetry index scores of original and repeat measures. ** denotes $p < 0.0001$; * denotes $p < 0.05$

<u>Landmark</u>	<u>Correlation</u>
ANS	0.704 **
Upper Central Incisors	0.777 **
Lower Central Incisors	0.736 **
Menton	0.673 **
Orbitale	0.372 *
Porion	0.787 **
Upper First Molar	0.776 **
Lower First Molar	0.770 **
Condyle	0.726 **
Coronoid	0.688 **
Gonion	0.667 **

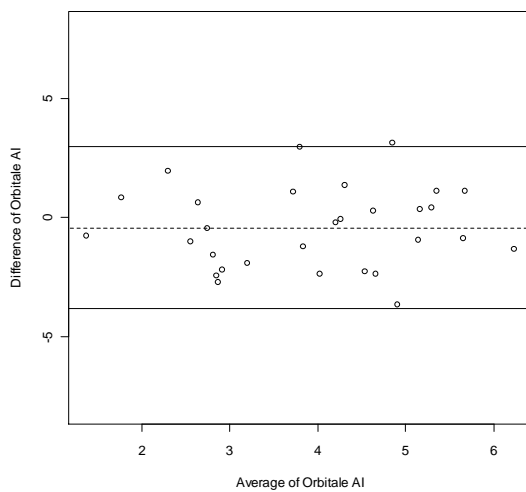
Table 6. Altman-Bland summary data analyzing agreement between initial and repeat measures of asymmetry index. No P-values were significant for a bias other than zero. Upper and lower agreements are for the 95% confidence level.

Landmark	Bias	Lower Agreement	Upper Agreement	P-Value
ANS	0.0067	-1.8520	1.8653	0.9695
Upper Central Incisors	-0.0133	-2.0656	2.0389	0.9449
Lower Central Incisors	0.0300	-2.3074	2.3674	0.8914
Menton	-0.1867	-3.1741	2.8008	0.5077
Orbitale	0.4228	-2.9107	3.7562	0.1838
Porion	-0.2394	-2.9676	2.4887	0.3539
Upper First Molar	-0.0487	-3.0948	2.9973	0.8649
Lower First Molar	0.1363	-3.5179	3.7904	0.6918
Condyle	0.0046	-2.6233	2.6326	0.9851
Coronoid	-0.4232	-3.3424	2.4960	0.1305
Gonion	0.2352	-4.0386	4.5089	0.5593

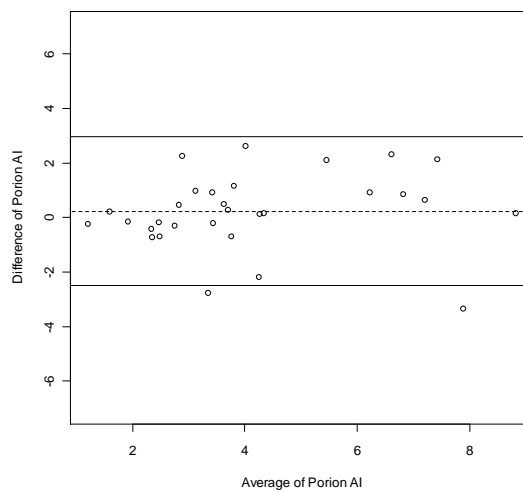
Figure 17. Altman-Bland plots of agreement of asymmetry index between the original data and the 30 patients who were re-assessed.



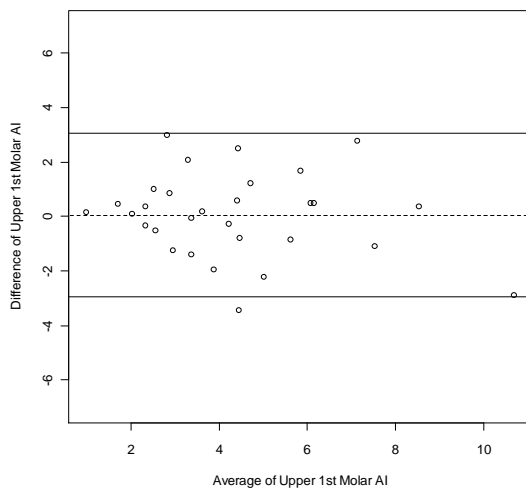
Altman Bland for Orbitale



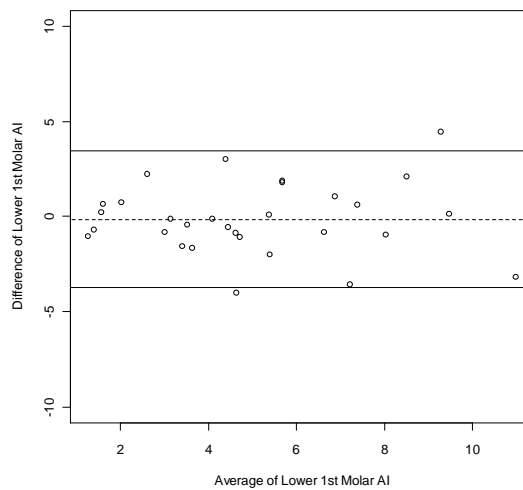
Altman Bland for Porion



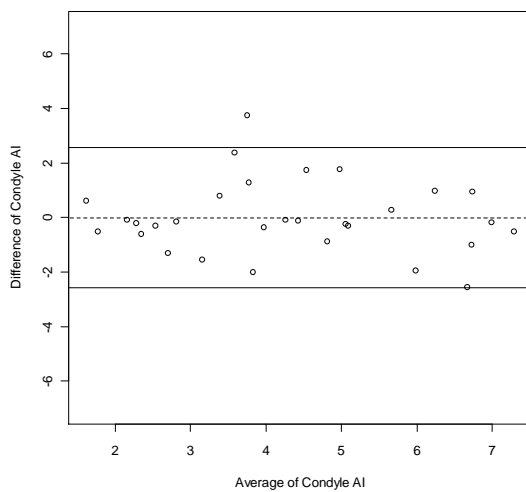
Altman Bland for Upper 1st Molar



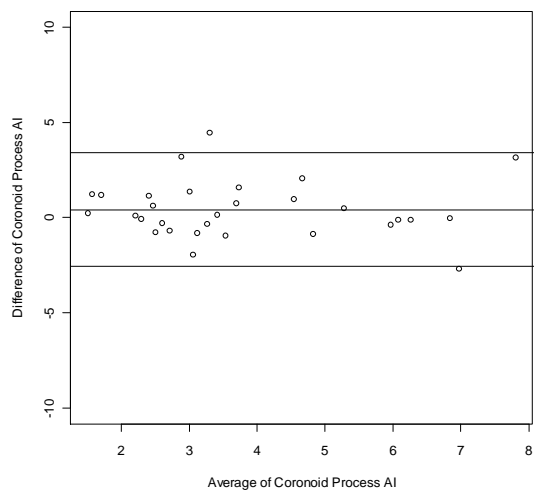
Altman Bland for Lower 1st Molar



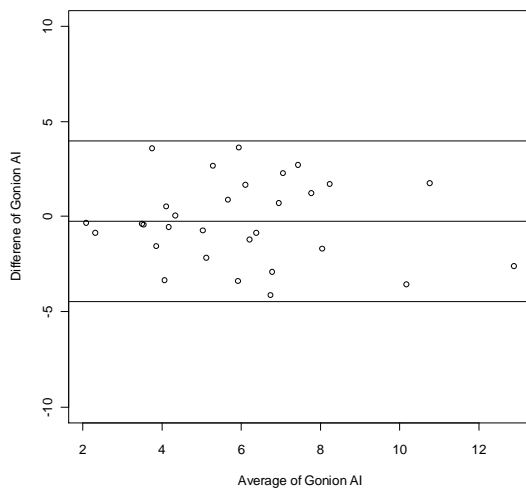
Altman Bland for Condyle



Altman Bland for Coronoid Process



Altman Bland for Gonion



Discussion

Assessing patient asymmetry is one of the many valuable diagnostic abilities that CBCT has the potential to greatly enhance. Previous methods of asymmetry assessment relied on multiple two dimensional images, such as lateral and posteroanterior cephalometric radiographs, to make assessments of skeletal asymmetry. These images are prone to distortions due to projection and head positioning errors.^{4,43,48} Therefore, using CBCT to assess asymmetry has great promise for clinical usefulness. Surgical treatment, for example, that correctly treats an underlying asymmetry will lead to better results than proceeding with an orthognathic treatment plan that may not address the chief area of asymmetry.³ Using a system such as the one described by Katsumata et al¹⁸ has the potential to unlock an area of diagnostic potential of CBCT films that has not yet been widely utilized.

The results of this study are insufficient to disprove either null hypothesis, that there is no relationship between skeletal asymmetry and ANB angle when patients are grouped into low or high ANB angles or that there is no relationship between skeletal asymmetry and ANB angle when ANB angle is investigated as a continuous variable. The data does not approach significance for any craniometric landmark in either situation. Looking at the scatter plots of asymmetry compared to ANB angle it appears that asymmetry index scores are randomly distributed among the patients. A skeletal class II is a result of either a deficient mandible or a maxillary anterior-posterior excess, or a combination of the two. Based on these results, it appears that the differential in jaw proportion in class II patients does not result in an increased proportion of asymmetry

compared to class I patients. A future research study could investigate three-dimensional asymmetry among groups of patients known to be asymmetric, such as class II subdivision patients or posterior crossbite patients, to test the sensitivity of this method.

The mean asymmetry index scores for each landmark in this study were compared to those found by Katsumata et al¹⁸ and compared by a two sample student t-test. All means in this study were higher than those in the previous study, with almost all at a $p < 0.05$ significance level. The main reason for this may be in the sample population. The current study utilized patients who presented for routine orthodontic care. These patient's caregivers were usually in some way dissatisfied with their child's dento-facial appearance. This contrasts markedly with the patients examined in the Katsumata study¹⁸, where they took a collection of 3000 CT images and selected a sample of 16 patients who were determined by three experienced radiologists to have no visible skeletal asymmetries on their CT scans prior to the asymmetry analysis and who presented for CT scans for diagnosis of conditions other than maxillofacial deformity.¹⁸ This population group represents an ideal with regards to symmetry. Under these conditions of patient inclusion it seems an increase in the level of asymmetry from the Katsumata study¹⁸ to the present study would be expected rather than a cause for concern, and the patients with malocclusion used in the present study appear to have greater levels of asymmetry than the ideal symmetrical population studied by Katsumata et al.¹⁸

This study examined reproducibility by reassessing the asymmetry index scores for 30 randomly selected patients from the original 70 patient group. Pearson correlation coefficients have low enough p values to demonstrate convincingly that the similarity

between the values of the two assessments are not due to chance. All are significant at $p < 0.0001$ level except orbitale. This will be discussed later in this study under sources of error.

Altman-Bland plots examined agreement of asymmetry index scores between the initial and reassessed patients. As the bias was not found to be significantly different than zero for any of the landmarks, there was no tendency for a repeat asymmetry index score to be either lower or higher than the original. There was, however, a range of agreement that varied from landmark to landmark. Looking at table 6, the landmark that had the best range of agreement was ANS. For this landmark the lower and upper limits of agreement for the asymmetry index were approximately -1.9 and 1.9. This means that for this landmark, a repeat measure of asymmetry index would be expected, with 95% certainty, to be within 1.9 units above or below the initial measure. Gonion, on the other hand, had the largest 95% agreement range. For gonion, the lower and upper limits of agreement were approximately -4.0 and 4.5. The other landmarks have 95% agreement ranges between ANS and Gonion, as shown in table 6.

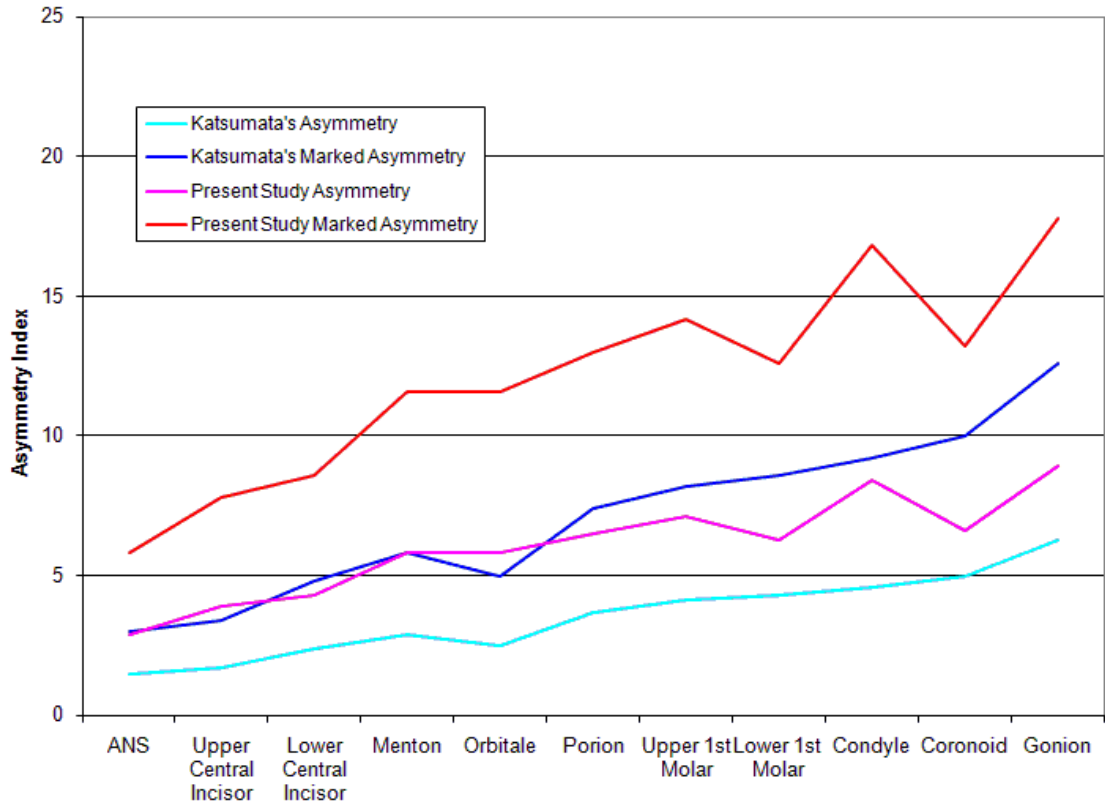
To determine if a landmark's asymmetry index reproducibility is sufficient for clinical assessment of asymmetry, it is important to consider how the asymmetry index is going to be used. Katsumata et al¹⁸ used the mean asymmetry index scores and standard deviations to establish ranges for symmetry, asymmetry, and marked asymmetry for a particular landmark. Their baseline for calling a landmark asymmetric was the mean for the landmark plus one standard deviation. For ANS, for example, this was an asymmetry index score of 1.5, anything above this was considered asymmetric. They defined a

landmark as markedly asymmetric if its asymmetry index score was twice the baseline level for asymmetry, for ANS this would be anything above 3.0 (see table 4 for mean values). For landmarks with higher mean asymmetry index scores and standard deviations, the cutoffs for diagnosing asymmetry are higher. Using the system of Katsumata et al¹⁸ and the range of agreement found in this study, the asymmetry index could vary on re-measure by enough to change the designation to the adjacent level of asymmetry for most landmarks, but no further. For example, if the patient is truly normal for a certain landmark, measurement error could push that landmark into the asymmetric category but not into the markedly asymmetric category. Also, for a patient that is truly markedly asymmetric for a certain landmark, measurement error could change that diagnosis to asymmetric but not to normal. For some of the landmarks, however, measurement error could change a truly symmetric landmark into a marked asymmetry and a truly marked asymmetry into a symmetric diagnosis. A summary of this is shown in table 7. The landmarks ANS, upper central incisor, menton, and orbitale are the most problematic when using this system for asymmetry diagnosis. A possible reason for this is the lower mean values of asymmetry index scores found for landmarks in the study by Katsumata et al¹⁸. A possible solution would be to use the higher mean asymmetry index scores and standard deviations found in the present study to establish boundaries for diagnosis of asymmetry and marked asymmetry for a particular landmark. This would create a situation where the asymmetry index would be less likely to misdiagnose an asymmetry, but more likely to miss a minor existing asymmetry. Figure 18 demonstrates graphically the boundaries for asymmetry and marked asymmetry diagnosis using the

method of Katsumata et al,¹⁸ as well as the new boundaries for diagnosis if means and standard deviations from the present study are used.

Table 7. Boundaries for asymmetry and marked asymmetry diagnosis by landmark according to system used by Katsumata et al ¹⁸ . Altman-Bland 95% agreement ranges are based on present study, and possible changes in diagnosis from symmetric to markedly asymmetric or from markedly asymmetric to symmetric are designated with an *.						
Landmark	Boundary: asymmetry diagnosis ¹⁸	Boundary: marked asymmetry diagnosis ¹⁸	Altman-Bland Lower agreement	Altman-Bland Upper agreement	Asymmetry boundary + upper agreement	Marked asymmetry boundary + lower agreement
ANS	1.5	3	-1.85	1.87	3.37 *	1.15 *
Upper central incisor	1.7	3.4	-2.07	2.04	3.74 *	1.33 *
Lower central incisor	2.4	4.8	-2.31	2.37	4.77	2.49
Menton	2.9	5.8	-3.17	2.80	5.70	2.63 *
Orbitale	2.5	5	-2.91	3.76	6.26 *	2.09 *
Porion	3.7	7.4	-2.97	2.49	6.19	4.43
Upper 1st molar	4.1	8.2	-3.09	3.00	7.10	5.11
Lower 1st molar	4.3	8.6	-3.52	3.79	8.09	5.08
Condyle	4.6	9.2	-2.62	2.63	7.23	6.58
Coronoid	5	10	-3.34	2.50	7.50	6.66
Gonion	6.3	12.6	-4.04	4.51	10.81	8.56

Figure 18. Katsumata et al¹⁸ asymmetry diagnosis boundaries compared to asymmetry diagnosis boundaries using the means and standard deviations from the current study.



Possible sources of error

Landmark identification errors are one of the main sources for error in a study such as this. Although the articles mentioned in the introduction of this study support the accuracy of landmark identification on CBCT images,^{9,21,26,41,50} there are extra difficulties to identifying landmarks in three dimensions on living human scans which can lead to errors. There may be reductions in image quality due to soft-tissue attenuation, metallic artifacts, and patient motion.³⁴ Because of these factors, landmark identification could have increased errors when using patient derived data compared to dry skull studies. Beyond this, there are certain landmarks that have proven more difficult to locate on CBCT images. A previous article identified orbitale as a difficult landmark to localize on certain patients.²⁶ This held true in the present study as orbitale had a markedly lower correlation coefficient than the other landmarks (see table 5). Part of the problem may have been with the definition of orbitale used in the present study. This study used the same definition of orbitale that the Katsumata study¹⁸ had used, defining it as the midpoint of the infraorbital margin. The problem arose in the subjectivity involved in determining where the midpoint was located. This inability to localize the medio-lateral position of orbitale lead to higher variability in measurements of the distance to the saggital plane, and consequently more variable asymmetry index scores. Possible solutions to this problem include using a definition that was presented Oliviera et al⁹, where orbitale is defined as the lateroinferior contour of the orbit, or a definition presented by S-H Park et al³³ who defined orbitale as the lowest point on the infraorbital

margin. Another possibility could be using an anatomical landmark such as the infra-orbital foramen or an orbital suture location that is visible on the CBCT image.

Another possible source of error in this study is in the creation of the three reference planes using the landmarks sella, nasion, and dent. All of these landmarks could fall under the term “fuzzy landmarks” as they require estimating the center of an anatomical region. Sella requires estimating the center of the pituitary fossa, nasion requires estimating the center of the nasofrontal suture, and dent requires estimating the center of the top of the epistropheus. All identification error of the reference landmarks leads to a built-in error for all asymmetry index measures. Even the relatively easy to identify landmark ANS has a range of 95% agreement for the asymmetry index of nearly two units in either direction. It is possible that this range of agreement for ANS asymmetry index scores is mostly due to variability in landmark identification of the reference landmarks and consequently variability in the reference planes. Ideally, a system of reference planes would be based upon easy to identify anatomic landmarks from which to base the reference planes which should increase the accuracy and reliability of this system.

Orienting the reference planes using Dolphin 3D created another source of error. The reference planes had to be manually oriented to pass through the center of each of the required reference landmarks. Dolphin 3D is able to identify how far the reference planes are located from the center of each of the landmarks, and this error was minimized by not allowing the reference planes to pass greater than 0.2mm away from the center of the landmarks before accepting the plane locations.

Dolphin 3D automatically calculated the linear distances from each landmark to each of the reference planes in millimeters. Because the linear measurement portion of the analysis was automated, it is not a likely source of further error in this study.

Conclusion

From this study, it appears that the differential in jaw proportion typical for class II skeletal patterns results in no more skeletal asymmetry than class I skeletal patterns. This study did not find a difference in skeletal asymmetry between class I and class II skeletal patients based on ANB angle using the asymmetry index developed by Katsumata et al¹⁸. There were no significant differences in groups of patients for asymmetry index when the patients were grouped into class I or class II ANB angles. There were also no trends in asymmetry index scores when ANB was investigated as a continuous variable. The mean asymmetry index scores for this study were significantly higher at most landmarks than those found in the previous study¹⁸. The reproducibility of asymmetry index values demonstrated high correlation but some landmark scores vary enough to impact a clinical diagnosis of asymmetry using the method suggested by Katsumata et al¹⁸.

References

1. Alavi DG, BeGole EA, Schneider BJ. Facial and dental arch asymmetries in Class II subdivision malocclusion. *Am J Orthod Dentofacial Orthop.* 1988;93(1):38-46.
2. Berco M, Rigali PH, Jr, Miner RM, DeLuca S, Anderson NK, Will LA. Accuracy and reliability of linear cephalometric measurements from cone-beam computed tomography scans of a dry human skull. *Am J Orthod Dentofacial Orthop.* 2009;136(1):17.e1-9; discussion 17-8.
3. Bishara SE, Burkey PS, Kharouf JG. Dental and facial asymmetries: a review. *Angle Orthod.* 1994;64(2):89-98.
4. BRODIE AG. Cephalometric roentgenology; history, techniques and uses. *J Oral Surg (Chic).* 1949;7(3):185-198.
5. Carlsson CA. Imaging modalities in x-ray computerized tomography and in selected volume tomography. *Phys Med Biol.* 1999;44(3):R23-56.
6. Chien PC, Parks ET, Eraso F, Hartsfield JK, Roberts WE, Ofner S. Comparison of reliability in anatomical landmark identification using two-dimensional digital cephalometrics and three-dimensional cone beam computed tomography in vivo. *Dentomaxillofac Radiol.* 2009;38(5):262-273.
7. Cook JT. Asymmetry of the cranio-facial skeleton. *Br J Orthod.* 1980;7(1):33-38.
8. Damstra J, Fourie Z, Huddleston Slater JJ, Ren Y. Accuracy of linear measurements from cone-beam computed tomography-derived surface models of different voxel sizes. *Am J Orthod Dentofacial Orthop.* 2010;137(1):16.e1-6; discussion 16-7.
9. de Oliveira AE, Cevidanes LH, Phillips C, Motta A, Burke B, Tyndall D. Observer reliability of three-dimensional cephalometric landmark identification on cone-beam computerized tomography. *Oral Surg Oral Med Oral Pathol Oral Radiol Endod.* 2009;107(2):256-265.
10. Grauer D, Cevidanes LS, Proffit WR. Working with DICOM craniofacial images. *Am J Orthod Dentofacial Orthop.* 2009;136(3):460-470.
11. Hassan B, van der Stelt P, Sanderink G. Accuracy of three-dimensional measurements obtained from cone beam computed tomography surface-rendered images

- for cephalometric analysis: influence of patient scanning position. *Eur J Orthod*. 2009;31(2):129-134.
12. Hesse KL, Artun J, Joondeph DR, Kennedy DB. Changes in condylar position and occlusion associated with maxillary expansion for correction of functional unilateral posterior crossbite. *Am J Orthod Dentofacial Orthop*. 1997;111(4):410-418.
 13. Hilgers ML, Scarfe WC, Scheetz JP, Farman AG. Accuracy of linear temporomandibular joint measurements with cone beam computed tomography and digital cephalometric radiography. *Am J Orthod Dentofacial Orthop*. 2005;128(6):803-811.
 14. Hounsfield GN. Computerized transverse axial scanning (tomography): Part I. Description of system. 1973. *Br J Radiol*. 1995;68(815):H166-72.
 15. Hwang HS, Hwang CH, Lee KH, Kang BC. Maxillofacial 3-dimensional image analysis for the diagnosis of facial asymmetry. *Am J Orthod Dentofacial Orthop*. 2006;130(6):779-785.
 16. Hwang HS, Youn IS, Lee KH, Lim HJ. Classification of facial asymmetry by cluster analysis. *Am J Orthod Dentofacial Orthop*. 2007;132(3):279.e1-279.e6.
 17. Janson G, de Lima KJ, Woodside DG, Metaxas A, de Freitas MR, Henriques JF. Class II subdivision malocclusion types and evaluation of their asymmetries. *Am J Orthod Dentofacial Orthop*. 2007;131(1):57-66.
 18. Katsumata A, Fujishita M, Maeda M, Ariji Y, Ariji E, Langlais RP. 3D-CT evaluation of facial asymmetry. *Oral Surg Oral Med Oral Pathol Oral Radiol Endod*. 2005;99(2):212-220.
 19. Komori M, Kawamura S, Ishihara S. Averageness or symmetry: which is more important for facial attractiveness? *Acta Psychol (Amst)*. 2009;131(2):136-142.
 20. Kowner R. Facial asymmetry and attractiveness judgment in developmental perspective. *J Exp Psychol Hum Percept Perform*. 1996;22(3):662-675.
 21. Kragsskov J, Bosch C, Gyldensted C, Sindet-Pedersen S. Comparison of the reliability of craniofacial anatomic landmarks based on cephalometric radiographs and three-dimensional CT scans. *Cleft Palate Craniofac J*. 1997;34(2):111-116.
 22. Lam PH, Sadowsky C, Omerza F. Mandibular asymmetry and condylar position in children with unilateral posterior crossbite. *Am J Orthod Dentofacial Orthop*. 1999;115(5):569-575.

23. Lascala CA, Panella J, Marques MM. Analysis of the accuracy of linear measurements obtained by cone beam computed tomography (CBCT-NewTom). *Dentomaxillofac Radiol.* 2004;33(5):291-294.
24. Lou L, Lagravere MO, Compton S, Major PW, Flores-Mir C. Accuracy of measurements and reliability of landmark identification with computed tomography (CT) techniques in the maxillofacial area: a systematic review. *Oral Surg Oral Med Oral Pathol Oral Radiol Endod.* 2007;104(3):402-411.
25. Ludlow JB, Davies-Ludlow LE, Brooks SL. Dosimetry of two extraoral direct digital imaging devices: NewTom cone beam CT and Orthophos Plus DS panoramic unit. *Dentomaxillofac Radiol.* 2003;32(4):229-234.
26. Ludlow JB, Gubler M, Cevidanes L, Mol A. Precision of cephalometric landmark identification: cone-beam computed tomography vs conventional cephalometric views. *Am J Orthod Dentofacial Orthop.* 2009;136(3):312.e1-10; discussion 312-3.
27. Ludlow JB, Laster WS, See M, Bailey LJ, Hershey HG. Accuracy of measurements of mandibular anatomy in cone beam computed tomography images. *Oral Surg Oral Med Oral Pathol Oral Radiol Endod.* 2007;103(4):534-542.
28. Maeda M, Katsumata A, Arijji Y, et al. 3D-CT evaluation of facial asymmetry in patients with maxillofacial deformities. *Oral Surg Oral Med Oral Pathol Oral Radiol Endod.* 2006;102(3):382-390.
29. Mah JK, Danforth RA, Bumann A, Hatcher D. Radiation absorbed in maxillofacial imaging with a new dental computed tomography device. *Oral Surg Oral Med Oral Pathol Oral Radiol Endod.* 2003;96(4):508-513.
30. Moller AP, Thornhill R. Bilateral symmetry and sexual selection: a meta-analysis. *Am Nat.* 1998;151(2):174-192.
31. Mongini F, Schmid W. Treatment of mandibular asymmetries during growth. A longitudinal study. *Eur J Orthod.* 1987;9(1):51-67.
32. Mozzo P, Procacci C, Tacconi A, Martini PT, Andreis IA. A new volumetric CT machine for dental imaging based on the cone-beam technique: preliminary results. *Eur Radiol.* 1998;8(9):1558-1564.
33. Park SH, Yu HS, Kim KD, Lee KJ, Baik HS. A proposal for a new analysis of craniofacial morphology by 3-dimensional computed tomography. *Am J Orthod Dentofacial Orthop.* 2006;129(5):600.e23-600.e34.

34. Periago DR, Scarfe WC, Moshiri M, Scheetz JP, Silveira AM, Farman AG. Linear accuracy and reliability of cone beam CT derived 3-dimensional images constructed using an orthodontic volumetric rendering program. *Angle Orthod.* 2008;78(3):387-395.
35. Pinsky HM, Dyda S, Pinsky RW, Misch KA, Sarment DP. Accuracy of three-dimensional measurements using cone-beam CT. *Dentomaxillofac Radiol.* 2006;35(6):410-416.
36. Pirttiniemi P, Kantomaa T, Lahtela P. Relationship between craniofacial and condyle path asymmetry in unilateral cross-bite patients. *Eur J Orthod.* 1990;12(4):408-413.
37. Pirttiniemi P, Raustia A, Kantomaa T, Pyhtinen J. Relationships of bicondylar position to occlusal asymmetry. *Eur J Orthod.* 1991;13(6):441-445.
38. Rhodes G, Proffitt F, Grady J, Sumich A. Facial Symmetry and the Perception of Beauty. *Psychonomic Bulletin & Review.* 1998;5(4):659-669.
39. Rhodes G. The evolutionary psychology of facial beauty. *Annu Rev Psychol.* 2006;57:199-226.
40. Rhodes G, Zebrowitz LA, Clark A, Kalick SM, Hightower A, McKay R. Do facial averageness and symmetry signal health? *Evol Hum Behav.* 2001;22(1):31-46.
41. Richtsmeier JT, Paik CH, Elfert PC, Cole TM, 3rd, Dahlman HR. Precision, repeatability, and validation of the localization of cranial landmarks using computed tomography scans. *Cleft Palate Craniofac J.* 1995;32(3):217-227.
42. Rose JM, Sadowsky C, BeGole EA, Moles R. Mandibular skeletal and dental asymmetry in Class II subdivision malocclusions. *Am J Orthod Dentofacial Orthop.* 1994;105(5):489-495.
43. Salzmann JA. Limitations of roentgenographic cephalometrics. *Am J Orthod Dentofacial Orthop.* 1964;50:169-188.
44. Samuels CA, Butterworth G, Roberts T, Graupner L, Hole G. Facial aesthetics: babies prefer attractiveness to symmetry. *Perception.* 1994;23(7):823-831.
45. Sarnas KV, Pancherz H, Rune B, Selvik G. Hemifacial microsomia treated with the Herbst appliance. Report of a case analyzed by means of roentgen stereometry and metallic implants. *Am J Orthod.* 1982;82(1):68-74.
46. Solberg WK, Bibb CA, Nordstrom BB, Hansson TL. Malocclusion associated with temporomandibular joint changes in young adults at autopsy. *Am J Orthod.* 1986;89(4):326-330.

47. Task Group on Control of Radiation Dose in Computed Tomography. Managing patient dose in computed tomography. A report of the International Commission on Radiological Protection. *Ann ICRP*. 2000;30(4):7-45.
48. Terajima M, Nakasima A, Aoki Y, et al. A 3-dimensional method for analyzing the morphology of patients with maxillofacial deformities. *Am J Orthod Dentofacial Orthop*. 2009;136(6):857-867.
49. Terajima M, Yanagita N, Ozeki K, et al. Three-dimensional analysis system for orthognathic surgery patients with jaw deformities. *Am J Orthod Dentofacial Orthop*. 2008;134(1):100-111.
50. Valeri CJ, Cole TM, 3rd, Lele S, Richtsmeier JT. Capturing data from three-dimensional surfaces using fuzzy landmarks. *Am J Phys Anthropol*. 1998;107(1):113-124.
51. Vazquez F, Grostic JD, Fonder AC, DeBoer KF. Eccentricity of the skull. Correlation with dental malocclusion. *Angle Orthod*. 1982;52(2):144-158.
52. Williams FL, Richtsmeier JT. Comparison of mandibular landmarks from computed tomography and 3D digitizer data. *Clin Anat*. 2003;16(6):494-500.